Journal Pre-proofs

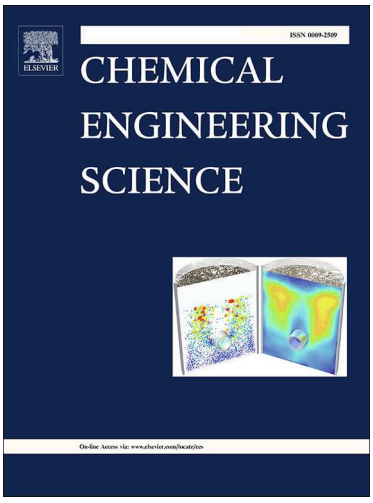

A new mathematical model for nucleation of spherical agglomerates by the immersion mechanism

Omid Arjmandi-Tash, Jonathan D. Tew, Kate Pitt, Rachel Smith, James D. Litster

PII: S0009-2509(19)30748-1
DOI: https://doi.org/10.1016/j.ces.2019.115258
Reference: CES 115258

To appear in: *Chemical Engineering Science*

Received Date: 5 July 2019
Revised Date: 23 September 2019
Accepted Date: 30 September 2019

Please cite this article as: O. Arjmandi-Tash, J.D. Tew, K. Pitt, R. Smith, J.D. Litster, A new mathematical model for nucleation of spherical agglomerates by the immersion mechanism, *Chemical Engineering Science* (2019), doi: http://dx.doi.org/10.1016/j.ces.2019.115258

*Corresponding author: James D. Litster, Email: james.litster@sheffield.ac.uk, Tel: +44 (0)114 2227592

A new mathematical model for nucleation of spherical agglomerates by the immersion mechanism

Omid Arjmandi-Tash, Jonathan D. Tew, Kate Pitt, Rachel Smith and James D. Litster*

EPSRC Future Continuous Manufacturing and Advanced Crystallisation Research Hub (CMAC),

Department of Chemical and Biological Engineering, University of Sheffield, UK

Abstract

Initial wetting of crystals by binder droplets is a key rate process in spherical agglomeration, however there are no models to predict the kinetics and formation of agglomerate nuclei. Two new mathematical models are introduced for agglomerate nucleation by an immersion mechanism; immersion rate limited model and collision rate limited model. The *agglomerate nucleation number* developed in this work predicts different regimes; *immersion rate limited*, *collision rate limited* and *intermediate*. In an immersion rate limited regime, agglomerate size increases with square root of time. In a collision rate limited regime, size increases linearly with time if the bulk crystal volume fraction, φ_{Pb}, is constant, or with an exponential decay rate for batch crystallisation with decreasing φ_{Pb}. The timescale for nucleation is less than ten minutes for a broad range of conditions, significantly less than most crystallisation timescales. These models have great promise for population balance modelling and spherical agglomeration optimisation.

Keywords: spherical agglomeration, immersion nucleation, immersion rate, collision rate, binder droplet, mathematical modelling

1. Introduction

Crystallisation has become an essential unit operation for the production, recovery and purification of products. The operation is widely used at a diverse range of scales and in a variety of different industries, including pharmaceuticals, bulk chemicals and catalysis, food processing, and cosmetics. The processing operations downstream from crystallisation are dependent upon not only the desired final product properties, but the quality of the product at the time of recovery. In this manner, it is rational for engineers to improve the identified key quality attributes as much as possible, either at, or during, this recovery step. In doing so, manufacturing processes can be simplified, and thereby become less energy intensive, require less operating capital, and improve overall product throughput. This process intensification is currently a major focus for several different industries, including the pharmaceuticals industry (Reay et al., 2008).

Spherical crystallisation is an umbrella term for a collective of techniques in which the product of interest is recovered through a crystallisation and then an agglomeration process; these steps can occur successively, in different unit operations, or simultaneously, in a single unit operation. Agglomeration is made possible by the addition of an immiscible solvent, termed the binder or bridging liquid. Three major techniques have been well documented within the literature; ammonia diffusion, quasi-emulsion solvent diffusion, and spherical agglomeration. Although one of these, spherical agglomeration, has been studied most broadly in research. Only this technique is

discussed in this paper, a full review of which has previously been presented by our group (Pitt et al., 2018).

In the pharmaceutical industry, where crystalline active pharmaceutical ingredients (APIs) are common, oral dosage forms are the preferred dispensary format. This requires APIs to have high compressibility and mechanical strength. Additionally, the dissolution profile and reactivity must also be considered to ensure that solid dosage forms perform as expected *in vivo* and have an acceptable shelf-life. The spherical agglomeration process is best applied to problematic, needle-like crystals, which are prone to breakage and, therefore, have poor compressibility (Amaro-González and Biscans, 2002; Kumar et al., 2008). Agglomerates produced by the technique are generally dense and spherical.

As both crystallisation and agglomeration procedures can be performed in tandem, it is possible to directly control the key quality attributes. Changes in the formulation parameters of the drug itself (e.g. additive or excipient addition etc.), or through modification of a variety of different process parameters (e.g. solid loading, shear etc.) can be used to achieve the desired attributes. Subsequently, the downstream processing required for solid dosage forms which meet the pre-determined criteria can be drastically reduced. Currently, granulation is used to control many of these product attributes. As agglomeration consolidates the crystal product, granulation is not required, and direct tabletting may be performed. Accordingly, the spherical agglomeration technique is a potential alternative to wet granulation, especially in the continuous manufacturing of pharmaceuticals (Amaro-González and Biscans, 2002; Peña et al., 2017; Pitt et al., 2018).

Spherical agglomeration was originally studied around fifty years ago, as a means of agglomerating a variety of different products. These studies investigated bulk materials related to natural resources including coal (Sirianni et al., 1969), graphite (Sutherland, 1962) and sand (Kawashima and Capes, 1976). The technique has broad appeal to both recover and consolidate products in a variety of different industries, especially those in which crystallisation is frequently used. Spherical agglomeration has also been investigated in high value products, particularly those in the pharmaceutical industry (Kawashima et al., 1982). Improvements in the properties of a variety of drugs have recently been reported, including lobenzarit disodium (Amaro-González and Biscans, 2002), mebendazole (Kumar et al., 2008) and aceclofenac (Usha et al., 2008), amongst others. Many studies have been experimentally orientated, and thus limited to observations on the influence of formulation and/or process parameters on product quality attributes, e.g. agglomerate size and distribution, porosity, mechanical strength etc. However, studies designed to specifically elucidate the mechanisms of the process are few, and subsequently a lack of robust models for performance prediction exist, which, ultimately, has hampered industrial adoption.

Many of the mechanisms in spherical agglomeration are thought to be analogous to wet granulation (Pitt et al., 2018) (see Fig. 1). In wet granulation, three key processes are often recognised and described (Iveson et al., 2001; Litster, 2016); (i) wetting and nucleation of particles by the binder; (ii) consolidation and growth of agglomerate nuclei; (iii) breakage and attrition of the nuclei. In a spherical agglomeration process, the binder liquid must be immiscible in the mother solution where the crystal particles are suspended. As in wet granulation, wetting of the crystal particles by the binder is thought

to occur through one of two separate mechanisms, depending upon the size ratio between these two entities (Schæfer and Mathiesen, 1996). If the binder droplets are smaller than the particles to be agglomerated, a distribution mechanism occurs. In this instance, crystals become 'coated' by droplets over time, which allows them aggregate together to form an initial agglomerate nucleus. If the binder droplets are larger than the particles to be agglomerated, an immersion mechanism occurs. Here, crystals penetrate inside the binder droplets over time and form an initial agglomerate nucleus within them. These observations for spherical agglomeration have been verified experimentally by several studies (Müller and Löffler, 1996; Orlewski et al., 2018; Subero-Couroyer et al., 2006). Immersion nucleation is favoured over distribution nucleation as agglomerates produced by this method tend to be more spherical, and denser with an easier control on size distribution (Subero-Couroyer et al., 2006).

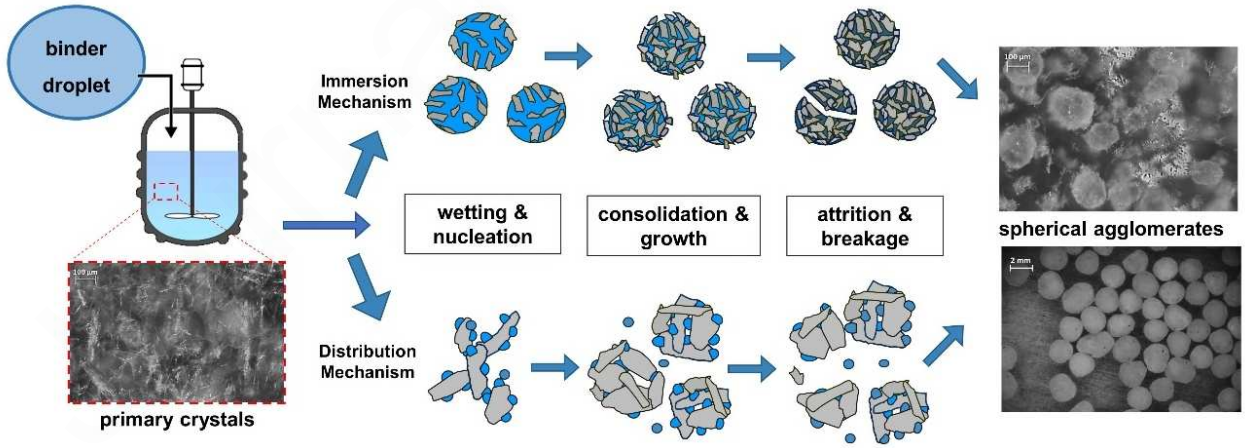

Fig. 1. Schematic of rate processes and possible mechanisms occurring during spherical agglomeration.

Of the studies which have taken a modelling approach in their work, population balance models to simulate agglomerate growth and consolidation is a favoured approach. Previously, agglomeration rate kernels have been successfully developed to model some of these rate processes. This includes growth by agglomerate-agglomerate collisions, or in the case of the distribution mechanism, crystal-crystal collisions, as well as the coalescence of agglomerate nuclei (Blandin et al., 2003; Blandin et al., 2005; David et al., 1991; David et al., 2003; Madec et al., 2003; Ochsenbein et al., 2015; Peña et al., 2017). The formation of liquid bridges between agglomerate nuclei, or between crystal particles, is often evaluated in this context. Whilst agglomerate-agglomerate collisions and subsequent coalescence of agglomerate nuclei happen in an immersion mechanism, it is not the predominant rate process during agglomerate formation. In the case of an immersion mechanism, the collision between crystal particles and binder droplets, and the immersion of crystals inside binder droplets or layering of agglomerate nuclei with crystals are the key rate processes. A model of crystals' immersion inside binder droplets in an immersion nucleation mechanism has been previously developed for the wet granulation process (Hounslow et al., 2009); however, no study has specifically looked at such mechanism in the context of spherical agglomeration. For spherical agglomeration models to be robust and predictive, it is important that all the rate processes, from wetting and nucleation, through to breakage and attrition, are considered and incorporated in the population balance model.

In this study, we evaluate the mechanism of immersion nucleation more closely, in terms of increases in agglomerate nuclei size with time due to layering; the acquisition of crystal particles suspended in the mother solution. Mathematical models are developed based

on mechanistic understanding and the physical phenomena happening during the process. From here, results are analysed based upon variations in common formulation and process parameters. Dimensionless groups are identified to determine the boundary between different regimes of the immersion nucleation mechanism. Critically, understanding these fundamental, initial mechanisms provides a solid foundation for future studies into the technique, which ultimately informs further model development.

2. Mathematical models for immersion nucleation

In order to form agglomerate nuclei in spherical agglomeration processes, firstly there should be collisions between crystal particles and binder droplets whilst the system is under agitation in the vessel. At the time of collision, based upon the impact velocity between binder droplets and crystal particles, as well as the surface tension forces at binder-mother solution interface, the following scenarios can arise:

1) the crystal particles are more wettable by binder liquid compared to the mother solution (i.e. the binder liquid/solid contact angle at three-phase binder liquid/mother solution/solid contact line, $\theta < 90^{O}$). Thus, the particles can penetrate inside the binder droplets regardless of the collision velocities and/or surface tension forces. However, the kinetics of the immersion of crystals inside the droplets can be limited by either collision, surface tension, or both of them. This scenario is desirable in spherical agglomeration process.

2) the particles are less wettable by binder liquid compared to the mother solution (i.e. the binder liquid/solid contact angle at three-phase binder liquid/mother solution/solid contact line, $\theta > 90^{O}$). Thus, the particles either stay at, or might rebound away from the interface between binder-mother solution due to interface resistance. Alternatively, the particles penetrate inside the binder droplets due to very high impacts, which overcomes the tension force at the interface (Lee and Kim, 2008).

Here, two mathematical models are presented for the kinetics of immersion of wettable particles by binder liquid described in the first scenario ($\theta < 90^{O}$). In both models, we assume that the further immersion of particles inside the binder droplet/agglomerate nucleus proceeds by the compressive force between the contacting particles. Therefore, the shell of the growing nucleus should have a constant packing volume fraction of particles (and thus liquid in between them). Here, we refer to this as the critical-packing liquid volume fraction, φ_{cp}. According to this assumption, the central part of the growing agglomerate nucleus should be composed of binder liquid only. The hypotheses for these models are shown in Fig. 2 as subsequent stages of agglomerate nucleus formation: initial impact of particles with a single binder droplet; coverage and initial shell formation composed of particles; expansion of the shell in a growing nucleus; complete filling by crystals inside the binder droplet. Such surface coverage of binder droplets with particles and subsequent immersion of particle inside the droplets were confirmed experimentally by Subero-Couroyer et al. (2006) and Bos (1983) for spherical agglomeration. This mechanism of immersion nucleation and the formation of shell and core were also

observed by X-ray tomography in the context of wet granulation process (Barera-Medrano et al., 2006; Bouwman et al., 2005).

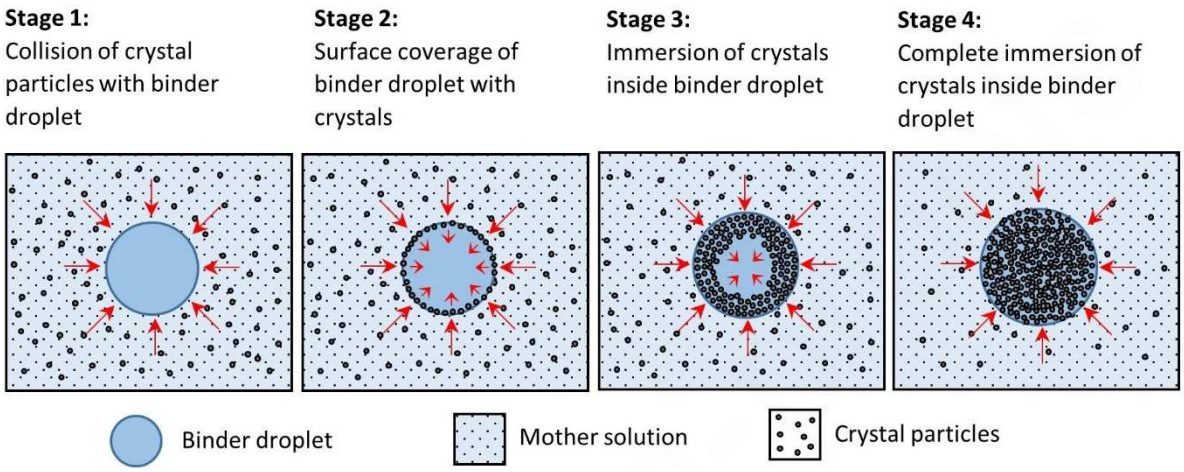

Fig. 2. Schematic of agglomerate immersion nucleation during spherical agglomeration.

In this instance, the agglomerate nucleation is controlled by the immersion rate of particles inside the binder droplet and/or the collision rate between binder droplets and crystal particles. In the first model, termed *immersion rate limited*, it is assumed that there is always a packed layer of stationary particles available on the surface of the binder droplets. We also assume the rate of immersion is only controlled by the wetting action (i.e. penetration of binder liquid in the packed layer according to Darcy's law, and the following suction of the particles inside the binder droplets). In the second model, termed *collision rate limited*, it is assumed that the suction of the particles due to the wetting action at the interface is so fast, the rate of agglomerate nucleation is limited only by the collision rate and the arrival of particles to the surface of binder droplets.

As a result of the stages shown in Fig. 2, the size of the agglomerate nucleus increases with the time of agglomeration. The evolution of the agglomerate size with time is captured using both immersion rate and collision rate limited models, and the timescale for complete agglomerate nucleation is determined using both models. Accordingly, dimensionless groups are identified to demarcate the boundary between different regimes for the process. Here, the problem is simplified in a planar geometry instead of a three-dimensional spherical geometry, as shown in Fig. 3. This allows us to analytically solve the derived equations, explicitly analyse the results based on the affecting parameters, and identify the dimensionless groups. $z=0$ corresponds to the centre of the binder droplet or the growing nucleus. $H_2(t)$ corresponds to the radius of the nucleus which evolves over time. $H_1(t)$ is the radius of the core which is composed of binder liquid only. $H_2(t) - H_1(t)$ defines the size of the shell with critical-packing liquid volume fraction (φ_{cp}), which also expands over the time. φ_{Pb} corresponds to the volume fraction of the crystal particles in the bulk mother liquid.

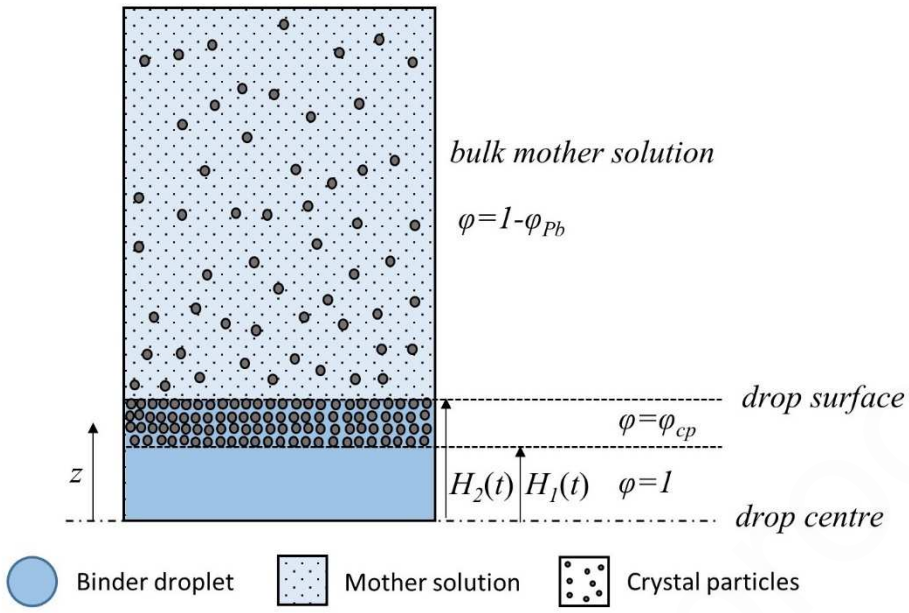

Fig. 3. Schematic of the system in planar geometry; $H_2(t)$ corresponds to the radius of the nucleus; $H_1(t)$ is the radius of the core; φ is the liquid volume fraction; φ_{cp} is the critical-packing liquid volume fraction; φ_{Pb} is the particles' volume fraction in the bulk mother solution.

2.1. Immersion rate limited model

In this model, it is assumed that the rate of collision between the particles and the binder droplets is always high, so there is always a packed layer of stationary particles available on the surface of the binder droplets. The rate of the immersion is found by the rate of imbibition of binder liquid in the packed layer, which is already wetted by the mother solution. In this section, we start by analysing the velocity profile for a flow in a cylindrical pipe, as a means of determining the rate of displacement of a non-wetting liquid (i.e. mother solution) by a wetting fluid (i.e. binder liquid) in a thin capillary. Later, we apply

this as a basis to model the kinetics of the imbibition of binder liquid in a packed layer of particles. Such a model has been previously developed by Hounslow et al. (2009) for the kinetics of immersion nucleation in the wet granulation process.

2.1.1 Displacement of a non-wetting liquid by a wetting fluid in a thin capillary

A velocity profile for a Newtonian fluid (e.g. binder liquid) in a cylindrical pipe of radius, R, with no-slip boundary condition is given by the following expression (Bird et al., 2007):

$$u(r) = \left(\frac{1}{4\mu_d} \left| \frac{dP}{dz} \right| \right) \left(R^2 - r^2 \right) \tag{1}$$

where, r is radial co-ordinate, $\left| \frac{dP}{dz} \right|$ is the pressure gradient for the flow and μ_d is the liquid viscosity. Hence, the flow rate, q (m^3/s), is expressed by: $q = \int_0^R 2\pi r u(r) dr$

$$q = \left(\frac{\pi}{8\mu_d} \left| \frac{dP}{dz} \right| \right) R^4 \tag{2}$$

The above equation allows determination of the average flux of the flow, Q (m/s):

$$Q = \frac{q}{\pi R^2} = \left(\frac{1}{8\mu_d} \left| \frac{dP}{dz} \right| \right) R^2 \tag{3}$$

Eq. (3) can be used to determine the rate of displacement of a non-wetting liquid by a wetting fluid in a thin capillary (Fig. 4):

$$Q = \frac{d\ell}{dt} = \left(\frac{1}{8\mu_d} \left| \frac{dP}{dz} \right| \right) R^2 \tag{4}$$

where the pressure gradient in the capillary can be given by:

$$\frac{dP}{dz} = \frac{2\gamma \cos\theta / R}{\ell} \tag{5}$$

Here, γ is the interfacial tension between the two immiscible liquids (i.e. binder liquid and mother solution), θ is the contact angle and ℓ is the length of displacement. Substitution of Eq. (5) into Eq. (4) gives:

$$\frac{d\ell}{dt} = \left(\frac{1}{4\mu_d} \frac{\gamma \cos\theta}{\ell} \right) R \tag{6}$$

or:

$$\ell \frac{d\ell}{dt} = \left(\frac{\gamma \cos\theta}{4\mu_d} \right) R \tag{7}$$

Solving the latter equation with the initial condition $\ell(t=0) = 0$ results in a well-known Washburn equation:

$$\ell(t) = \left(\frac{R\gamma \cos\theta}{2\mu_d} t \right)^{1/2} \tag{8}$$

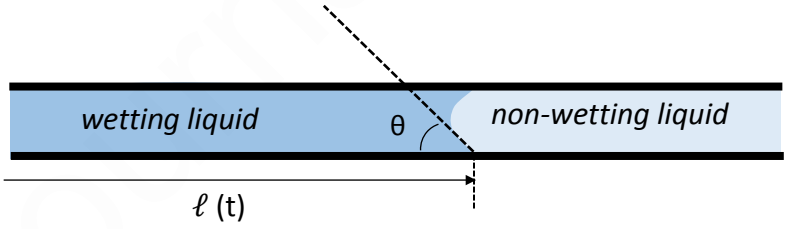

Fig. 4. Displacement of a non-wetting liquid by a wetting fluid in a thin capillary

2.1.2. Immersion rate of primary crystals inside binder droplets

In the case of a packed layer of crystal particles, we can use the well-known Darcy's equation to calculate the immersion rate:

$$Q_{imm}=\frac{\kappa}{\mu_d}\frac{\Delta P}{\Delta z}, \tag{9}$$

where κ is the permeability; μ_d is the binder liquid viscosity and the driving force for imbibition ($\Delta P/\Delta z$) is:

$$\left|\frac{\Delta P}{\Delta z}\right| = \frac{\frac{2\gamma\cos\theta}{R_{eff}}}{H_2(t)-H_1(t)}, \tag{10}$$

Here, $H_2(t)-H_1(t)$ and R_{eff} are the size and the effective radius of the pores for the packed layer of the particles, respectively. White (1982) proposed that R_{eff} may be defined as:

$$R_{eff} = \frac{2}{S_v}\left(\frac{\varphi_{cp}}{1-\varphi_{cp}}\right) \tag{11}$$

where S_v is the specific surface area per unit volume and φ_{cp} is the critical-packing liquid volume fraction. Substituting Eq. (11) into Eq. (10) results in:

$$\left|\frac{\Delta P}{\Delta z}\right| = \frac{S_v\gamma\cos\theta}{H_2(t)-H_1(t)}\frac{1-\varphi_{cp}}{\varphi_{cp}}, \tag{12}$$

On the other hand, the permeability, κ, in Eq. (9) can be given by the Kozeny-Carman equation:

$$\kappa = \frac{1}{KS_v^2}\frac{\varphi_{cp}^{\ 3}}{(1-\varphi_{cp})^2} \tag{13}$$

where K is known as Kozeny's constant and is generally ≈ 5. $S_v=6/\Psi D_p$, Ψ is the sphericity factor of crystal particles and D_p is the Sauter mean particle diameter.

Substituting Eqs. (12) and (13) into Eq. (9) and replacing S_v and K results in:

$$Q_{imm} = \varphi_{cp} \frac{d(H_2(t) - H_1(t))}{dt} = \frac{\Psi D_p \gamma \cos\theta}{30\mu_d} \frac{1}{H_2(t) - H_1(t)} \frac{\varphi_{cp}^{\ 2}}{(1-\varphi_{cp})} \tag{14}$$

The solution of the above equation leads to the following equation for the layer of immersed crystals inside the binder droplet over the time:

$$(H_2(t) - H_1(t)) = \left(\frac{\Psi D_p \gamma \cos\theta}{15\mu_d} \frac{\varphi_{cp}}{(1-\varphi_{cp})} t \right)^{1/2} \tag{15}$$

Considering the binder liquid conservation, the size of the agglomerate nucleus at a given time can be found as:

$$H_2(t) = \frac{D_d}{2} + \left(\frac{\Psi D_p \gamma \cos\theta}{15\mu_d} (1-\varphi_{cp}) \varphi_{cp} t \right)^{1/2} \tag{16}$$

where D_d is the size of the binder droplet.

The maximum size that a binder droplet with an initial size of D_d can expand during a agglomerate nucleation process is $H_2^{max} = (D_d/2)/\varphi_{cp}$. At this point the whole volume of the agglomerate nucleus is filled with primary crystals with the critical-packing liquid volume fraction, $\varphi_{cp.}$. Substituting the latter in Eq. (16) gives the timescale for complete immersion of crystals inside the binder droplet limited by immersion rate:

$$t_{imm} = \frac{15\mu_d D_d^{\ 2}}{4\Psi D_p \gamma \cos\theta} \frac{(1-\varphi_{cp})}{\varphi_{cp}^3} \tag{17}$$

Eq. (17) is very similar to the timescale found by Hounslow et al. (2009) for the kinetics of immersion nucleation driven by surface tension in the wet granulation process. However, here the surface tension is replaced by the interfacial tension between the

binder liquid and mother solution, and an sphericity factor is introduced for the particles as spherical agglomeration is mostly applied to non-spherical crystalline particles.

Here, we introduce the following dimensionless co-ordinate and time:

$$\zeta \to z/(\frac{D_d}{2}) \tag{18.a}$$

$$\tau_{imm} \to t/t_{imm} \tag{18.b}$$

where $D_d/2$ (i.e. $H_2(t=0)$) is the initial radius of the agglomerate nuclei and t_{imm} is the timescale for complete immersion defined by Eq. (17). By substitution of these variables, the dimensionless size of the immersed crystal layer and the agglomerate nucleus can be found by the following equations:

$$(\zeta_2(\tau_{imm}) - \zeta_1(\tau_{imm})) = \frac{\tau_{imm}^{1/2}}{\varphi_{cp}} \tag{19}$$

$$\zeta_2(\tau_{imm}) = 1 + \frac{(1-\varphi_{cp})}{\varphi_{cp}} \tau_{imm}^{1/2} \tag{20}$$

2.2. Collision rate limited model

The immersion rate limited model is only valid if we assume that there is always a packed layer of primary crystals with critical-packing liquid volume fraction of φ_{cp} at the surface of binder droplets. However, the process may be limited by the arrival of crystals at the surface of the growing nucleus, especially if the collision rate of binder droplets and particles is not sufficiently high.

The collision rate of small crystals with a binder droplet, or the flux of particles towards the binder droplet surface in a turbulent flow, can be found by (Kuboi et al., 1984):

$$Q_{coll} = \alpha\left[u(D_p)^2 + u(D_d)^2\right]^{1/2}\varphi_{Pb} \tag{21}$$

where $u(D_p)$ and $u(D_d)$ are the particle-mother solution and binder droplet-mother solution relative velocities, respectively. φ_{Pb} defines the crystal volume fraction in the bulk mother solution. α is the target efficiency and represents the fraction of crystals in the fluid volume swept by the binder droplet which will impinge on the droplet (see Fig. 5):

$$\alpha = X/D_d \cong N_{sep} = \frac{u_t(D_p)\left[u(D_p)^2 + u(D_d)^2\right]^{1/2}}{gD_d} = \frac{\xi D_p}{2gD_d}\left[u(D_p)^2 + u(D_d)^2\right]^{1/2} \tag{22}$$

where X is a length scale of flow around the binder droplet, as shown in Fig. 5, in which all particles carried by the fluid are collected on the binder droplet; N_{sep} is the separation number; $u_t(D_P)$ is crystal particles terminal velocity; g is the gravitational acceleration; and ξ and $u(D_i)$ are defined as (i stands for both p, crystal particle and d, binder droplet/agglomerate nucleus):

$$\xi = \left[\frac{32}{225}\frac{(\rho_p - \rho_L)^2 g^2}{\rho_L \mu_L}\right]^{1/3},\ u(D_i) = \left[\frac{(|\rho_i - \rho_L|)^3}{200\rho_L\mu_L(2\rho_i + \rho_L)}\right]^{1/2} D_i^{3/5}\varepsilon^{2/5} \tag{23}$$

where ρ_p is the particle skeletal density; ρ_L and μ_L are density and viscosity of mother solution, respectively; ε is the average energy dissipated per unit of suspension mass.

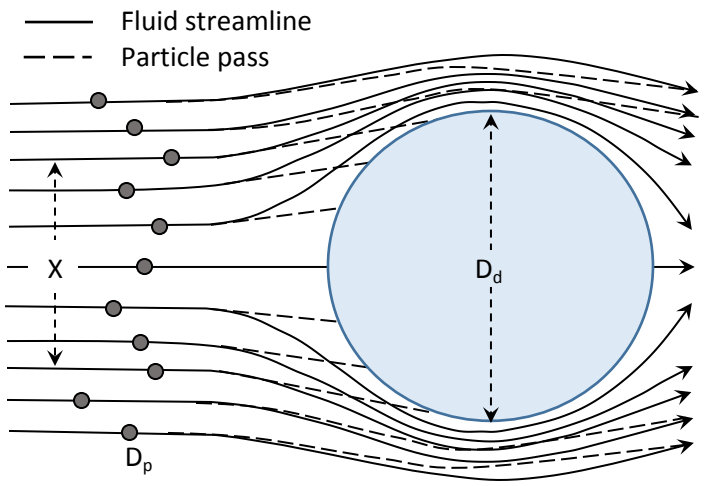

Fig. 5. Schematic of binder droplet and particle collision

If we assume that the immersion of particles inside the binder droplets is limited by the arrival of crystals at the surface of the growing nucleus, then the binder liquid and solid particles conservation gives the following equation for the change of interfaces and particle shell inside the binder droplets:

$$\frac{d(H_2(t)-H_1(t))}{dt}=\frac{Q_{coll}}{(1-\varphi_{cp})} \tag{24}$$

If the crystal volume fraction in the bulk mother solution is constant and neglecting the change of $u(D_d)$ over the time of agglomerate nucleation, solution of Eq. (24) yields:

$$H_2(t)-H_1(t)=\frac{\alpha\left[u(D_p)^2+u(D_d)^2\right]^{1/2}\varphi_{Pb}}{(1-\varphi_{cp})}t \tag{25}$$

Considering the binder liquid conservation, the size of the agglomerate nucleus can be found over time as:

$$H_2(t) = \frac{D_d}{2} + \alpha\left[u(D_p)^2 + u(D_d)^2\right]^{1/2}\varphi_{Pb}t \tag{26}$$

and the timescale for complete immersion of crystals inside the binder droplet limited by the collision rate can be calculated by:

$$t_{coll\_cont} = \frac{D_d(1-\varphi_{cp})}{2\alpha\left[u(D_p)^2 + u(D_d)^2\right]^{1/2}\varphi_{Pb}\varphi_{cp}} \tag{27}$$

We can use the following dimensionless co-ordinate and time:

$$\zeta \rightarrow z/(\frac{D_d}{2}) \tag{28.a}$$

$$\tau_{coll\_cont} \rightarrow t/t_{coll\_cont} \tag{28.b}$$

where t_{coll_cont} is the timescale for collision rate limited immersion defined by Eq. (27). By substitution of these variables, the dimensionless size of the immersed crystal layer and the agglomerate nucleus can be found by the following equations:

$$(\zeta_2(\tau_{coll\_cont}) - \zeta_1(\tau_{coll\_cont})) = \frac{\tau_{coll\_cont}}{\varphi_{cp}} \tag{29}$$

$$\zeta_2(\tau_{coll\_cont}) = 1 + \frac{(1-\varphi_{cp})}{\varphi_{cp}}\tau_{coll\_cont} \tag{30}$$

In a continuous, well mixed system at steady state (mixed-suspension, mixed-product removal, MSMPR), the crystal volume fraction in the bulk mother solution remains constant and Eqs. (25)-(30) represent the changes to a single agglomerate nucleus in the system. When used in conjunction with a mass balance and population balance for the system, they will give an expression for the size and crystal content distribution of nuclei in the agglomerator.

In a batch agglomeration system, the crystal volume fraction in the bulk mother solution decreases due to immersion inside the binder droplets. In this case we can write the following equation based on the conservation of solid particles (see Appendix A):

$$\varphi_{Pb}(t) = \varphi_{Pb0}(1 - \frac{2TBSR}{D_d}(1-\varphi_{cp})(H_2(t) - H_1(t))) \tag{31}$$

where φ_{Pb0} is the initial crystal volume fraction in the bulk mother solution. $TBSR$ is the True volumetric Binder liquid-to-Solid Ratio and it considers the true volume of binder liquid which stays as a separate phase within the suspension in the form of droplets. In the case of partial miscibility of binder liquid in the mother solution, $TBSR$ value deviates from the volumetric ratio of the *initially* added binder liquid to the crystal particles.

Substituting Eq. (31) into the collision rate, Eq. (21), and solving Eq. (24) leads to the following equations for the size of the immersed crystal layer inside binder droplets and the size of the agglomerate nuclei, respectively:

$$H_2(t) - H_1(t) = \frac{D_d}{2TBSR(1-\varphi_{cp})}\left(1 - \exp(-\frac{2\alpha\left[u(D_p)^2 + u(D_d)^2\right]^{1/2}\varphi_{Pb0}TBSR}{D_d}t)\right) \tag{32}$$

$$H_2(t) = \frac{D_d}{2} + \frac{D_d}{2TBSR}\left(1 - \exp(-\frac{2\alpha\left[u(D_p)^2 + u(D_d)^2\right]^{1/2}\varphi_{Pb0}TBSR}{D_d}t)\right) \tag{33}$$

The timescale for complete immersion of crystals inside the binder droplets in a batch agglomeration system can be calculated by:

$$t_{coll\_bat} = \frac{D_d}{2\alpha\left[u(D_p)^2 + u(D_d)^2\right]^{1/2}\varphi_{Pb0}TBSR} Ln(\frac{1}{1 - TBSR\dfrac{(1-\varphi_{cp})}{\varphi_{cp}}}) \tag{34}$$

To use Eq. (34), the value of $TBSR\frac{(1-\varphi_{cp})}{\varphi_{cp}}$ should be between 0 and 1 and, accordingly, the $TBSR$ value should always be lower than $\frac{\varphi_{cp}}{(1-\varphi_{cp})}$. A $TBSR$ value higher than $\frac{\varphi_{cp}}{(1-\varphi_{cp})}$ shows that there are not enough particles in the bulk mother liquid to fill the whole volume of binder droplets with a particle volume fraction of $(1\text{-}\ \varphi_{cp})$. In this case, the timescale for complete immersion of crystals inside the binder droplets will be infinite using both collision rate limited and immersion rate limited models.

Using the following dimensionless co-ordinate and time,

$$\zeta \to z/(\frac{D_d}{2}), \quad \tau_{coll\_bat} \to t/t_{coll\_bat} \tag{35}$$

the dimensionless size of the immersed crystal layer and the agglomerate nucleus can be found by the following equations, respectively:

$$\zeta_2(\tau_{coll\_bat}) - \zeta_1(\tau_{coll\_bat}) = \frac{1}{TBSR(1-\varphi_{cp})}\left(1-(1-TBSR\frac{(1-\varphi_{cp})}{\varphi_{cp}})^{\tau_{coll\_bat}}\right) \tag{36}$$

$$\zeta_2(\tau_{coll\_bat}) = 1+\frac{1}{TBSR}\left(1-(1-TBSR\frac{(1-\varphi_{cp})}{\varphi_{cp}})^{\tau_{coll\_bat}}\right) \tag{37}$$

2.3. Dimensionless groups and different regimes of the process

A summary of all the assumptions utilised in developing immersion rate and collision rate limited models is presented in Table 1.

Table 1. A summary of all the assumptions applied in mathematical models

Model	Assumptions
Both immersion rate and collision rate limited models	• Crystal particles more wettable by binder liquid compared to the mother solution, $\theta < 90^{O}$ • Immersion of particles inside the binder droplet/agglomerate nucleus by the compressive force between the contacting particles • Formation of core and shell with liquid volume fraction of 1 and φ_{cp}, respectively, inside a growing agglomerate nucleus, • A planar geometry instead of a three-dimensional spherical geometry
Immersion rate limited model	• A packed layer of stationary particles available on the surface of the binder droplets • Agglomerate nucleation limited by the immersion rate of particles inside binder droplets • Immersion rate found by the rate of imbibition of binder liquid in the packed layer through Darcy's law • Permeability of the packed layer given by the Kozeny-Carman equation
Collision rate limited model	• Extremely fast immersion of particles inside binder droplets • Agglomerate nucleation limited by the collision rate between particles and binder droplets • Sizes of binder droplets and crystal particles larger than the turbulent microscale of Kolomogorov

	• Negligible change of binder droplet-mother solution relative velocity, $u(D_d)$, over nucleation time
Constant φ_{Pb} (continuous, well mixed, steady state) agglomeration system	• Constant crystal volume fraction in the bulk mother solution
batch agglomeration system	• Decrease in crystal volume fraction in the bulk mother solution due to immersion inside binder droplets

The kinetics of agglomerate nucleation in the case of the immersion mechanism can be limited either by;

- Immersion rate of particles inside binder droplets due to the surface tension forces at the binder-mother solution interface according to Eq. (14), if there is always a packed layer of particles on the surface of the binder droplets;
- Or by the collision rate and arrival of particles to the binder droplet surfaces according to Eq. (24), if the immersion of particles inside binder droplets due to surface tension forces is extremely fast.

In some cases, the system can be limited by both the immersion rate and the collision rate. In order to find the boundary between the different regimes for the process we can obtain a dimensionless group by calculating the ratio between the timescales for complete agglomerate nucleation limited by the immersion rate and the collision rate:

$$\frac{t_{imm}}{t_{coll\_cont}} = \frac{Ca\varphi_{Pb}}{\lambda} = AgNu \tag{38}$$

or

$$\frac{t_{imm}}{t_{coll\_bat}} = AgNu \frac{TBSR\frac{(1-\varphi_{cp})}{\varphi_{cp}}}{Ln(\frac{1}{1-TBSR\frac{(1-\varphi_{cp})}{\varphi_{cp}}})} \tag{39}$$

where $AgNu$ is *agglomerate nucleation number* and Ca is a modified capillary number defined by:

$$Ca = \frac{15\mu_d\alpha\left[u(D_p)^2 + u(D_d)^2\right]^{1/2}}{2\Psi\gamma\cos\theta\varphi_{cp}^2} \tag{40}$$

and λ is the ratio of the particle size to the binder droplet size defined as follows:

$$\lambda = \frac{D_p}{D_d} \tag{41}$$

For a system with an agglomerate nucleation number, $AgNu$, significantly larger than one (e.g. >10^2), the process of agglomerate nucleation is limited by the immersion rate. Thus, the size of agglomerate nuclei over the time can be found by Eqs. (16) and (20). On the other hand, if the agglomerate nucleation number, $AgNu$, is significantly lower than one (e.g. <0.01), the process is controlled by the collision and arrival of the particles at the

binder droplet surfaces. Thus, the size of agglomerate nuclei can be obtained by Eqs. (26) and (30), or (33) and (37). However, for a system with $AgNu$ close to one, the agglomerate nucleation can be limited by both immersion rate and collision rate, and thus the size of agglomerate nuclei must be found by a combination of both models. Three different model systems will be presented in the next section to discuss the conditions and the behavior of immersion kinetics for each aforementioned regime.

3. Results and discussion

To investigate the change of the size of the agglomerate nucleus using the developed models, the size can be scaled to the range (0 ,1) as:

$$\psi(\tau) = \frac{H_2(t) - (D_d / 2)}{(D_d / 2)/\varphi_{cp} - (D_d / 2)} = \frac{\zeta_2(\tau) - 1}{1/\varphi_{cp} - 1} \tag{42}$$

where ζ_2 can be found by Eq. (20) for an immersion rate limited model or Eqs. (30) and (37) for a collision rate limited model. Here, ψ can also be treated as a dimensionless volume since the volume of agglomerate nucleus in the planar geometry is proportional to its size. Fig. 6 shows the dimensionless volume, ψ, as a function of dimensionless time, τ, for each model. Calculating ψ results in:

$$\psi_{imm}(\tau_{imm}) = \tau_{imm}^{1/2} \tag{43}$$

for the immersion rate limited model, and:

$$\psi_{coll\_cont}(\tau_{coll\_cont}) = \tau_{coll\_cont} \tag{44}$$

$$\psi_{coll\_bat}(\tau_{coll\_bat}) = \frac{\varphi_{cp}}{(1-\varphi_{cp})TBSR}\left(1-(1-TBSR\frac{(1-\varphi_{cp})}{\varphi_{cp}})^{\tau_{coll\_bat}}\right) \quad (45)$$

for collision rate limited models. As can be seen in Fig. 6(a) and the above equations, the dimensionless volume, ψ, is only a function of dimensionless time, τ, for both the immersion rate limited model (i.e. square root) and the collision rate limited model in constant φ_{Pb} (continuous, well mixed, steady state) agglomeration system (i.e. linear function). However, for a collision rate limited model in a batch agglomeration system where φ_{Pb} decreases over agglomerate nucleation time, ψ is also a function of $TBSR$ and φ_{cp}. This reduction in the volume fraction of crystals in the bulk mother solution, φ_{Pb}, is due to the immersion of crystals inside binder droplets during agglomerate nucleation.

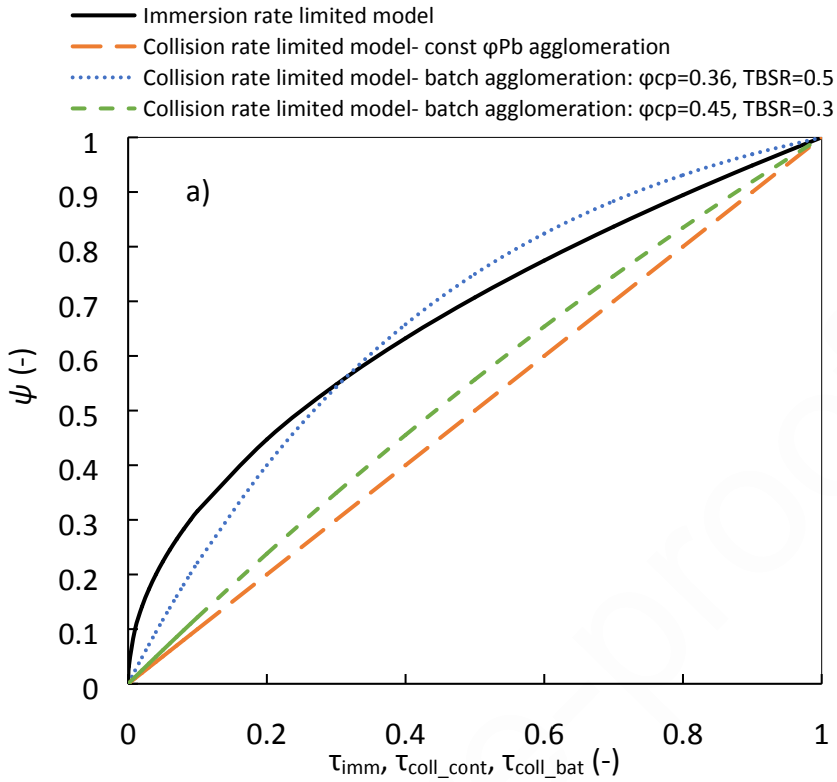
Immersion rate limited model
Collision rate limited model- const φPb agglomeration
Collision rate limited model- batch agglomeration: φcp=0.36, TBSR=0.5
Collision rate limited model- batch agglomeration: φcp=0.45, TBSR=0.3
a)
ψ (-)
0
0.1
0.2
0.3
0.4
0.5
0.6
0.7
0.8
0.9
1
0
0.2
0.4
0.6
0.8
1
τimm, τcoll_cont, τcoll_bat (-)

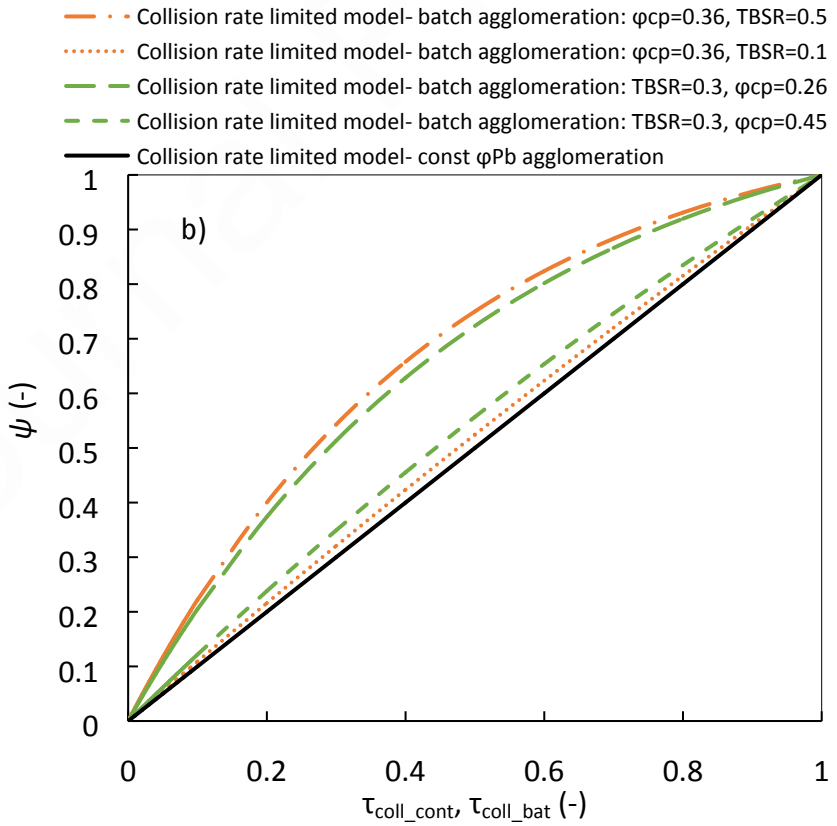
Collision rate limited model- batch agglomeration: φcp=0.36, TBSR=0.5
Collision rate limited model- batch agglomeration: φcp=0.36, TBSR=0.1
Collision rate limited model- batch agglomeration: TBSR=0.3, φcp=0.26
Collision rate limited model- batch agglomeration: TBSR=0.3, φcp=0.45
Collision rate limited model- const φPb agglomeration
b)
ψ (-)
0
0.1
0.2
0.3
0.4
0.5
0.6
0.7
0.8
0.9
1
0
0.2
0.4
0.6
0.8
1
τcoll_cont, τcoll_bat (-)

Fig. 6. Dimensionless volume, ψ, as a function of dimensionless time, τ for a) the immersion rate limited model and collision rate limited models (constant φ_{Pb} and batch systems); b) collision rate limited models for a batch system with various φ_{cp} and $TBSR$ values and a constant φ_{Pb} (continuous, well mixed, steady state) system. Note that the timescale is different for each model as shown in Eqs. (17), (27) and (34).

The reduction of crystals in the bulk mother solution is negligible during agglomeration if either the solid to binder ratio (i.e. $1/TBSR$) or the critical-packing liquid volume fraction inside binder droplets, φ_{cp}, are very high in the system. In these cases, the result of the collision rate limited model for a batch agglomeration system with variable φ_{Pb} tends to be identical to that of a prediction for a continuous, well mixed, steady state agglomeration system with constant φ_{Pb}. As a result, the change of nuclei size and volume over time will be relatively linear. This behavior can be seen in Fig. 6(b).

3.1. Different regimes of agglomerate nucleation

In order to discuss the conditions for using the developed immersion rate and collision rate limited models, and the behavior of the agglomerate nucleation in each model, three different model systems for spherical agglomeration with different formulation properties and process conditions are presented in Table 2. The model systems correspond to the agglomeration of needle-like crystals of lovastatin suspended in water as a mother solution (Perciballi, 2017). Heptane is used in model system 1 as binder liquid; average energy dissipation, ε, and bulk volume fraction of crystals, φ_{Pb}, are reasonably low in this

system. Model systems 2 and 3 use more viscous binder liquids with low interfacial tensions. The average energy dissipation, ε, in model system 2 is much higher than model systems 1 and 3. All the values for formulation and process parameters used in model systems are physically realistic and practical during a spherical agglomeration process. α, ξ, $u(D_p)$ and $u(D_d)$ are calculated by Eqs. (22) and (23) using the parameters of each model system. The timescales of agglomerate nucleation for the immersion rate limited model, t_{imm}, and the collision rate limited model, t_{coll_cont}, and t_{coll_bat} are obtained according to Eqs. (17), (27) and (34), respectively. Finally, the dimensionless parameters, Ca, λ, $AgNu$, are calculated for each model system using Eqs. (38)-(41).

Table 2. Three different model systems for spherical agglomeration with different formulation/process parameters along with the calculated timescales and dimensionless numbers. The model systems correspond to the agglomeration of needle-like crystals of lovastatin suspended in water. Model system 1 uses heptane as binder liquid. Model systems 2 and 3 use more viscous binder liquids with low interfacial tensions. Average energy dissipation, ε, and bulk volume fraction of crystals, φ_{Pb}, in model system 1 are lower than the other model systems. The average energy dissipation, ε, in model system 2 is much higher than model systems 1 and 3.

	Model system		
Formulation/process parameters	1	2	3
D_p (m)	5.00E-05	5.00E-05	5.00E-05
D_d (m)	2.00E-04	2.00E-04	2.00E-04

μ_d (Pa.s)	3.76E-04	1	1
μ_L (Pa.s)	8.90E-04	8.90E-04	8.90E-04
γ (N/m)	0.05	0.01	0.02
θ (°)	60	80	80
ρ_p (kg/m^3)	1100	1100	1100
ρ_d (kg/m^3)	684	684	684
ρ_L (kg/m^3)	1000	1000	1000
ε (m^2/s^3)	0.01	5	0.02
Ψ (-)	0.43	0.43	0.50
φ_{cp} (-)	0.36	0.36	0.36
φ_{Pb} (-)	0.045	0.18	0.18
$TBSR$ (-)	0.55	0.30	0.30
Calculated parameters			
α (-)	5.66E-03	6.80E-02	7.47E-03
ξ (1/s)	53.54	53.54	53.54
$u(D_p)$ (m/s)	5.52E-04	6.62E-03	7.28E-04
$u(D_d)$ (m/s)	8.27E-03	9.94E-02	1.09E-02
Timescales			
t_{imm} (s)	1.43E-03	55.11	23.70
t_{coll_cont} (s)	83.28	0.14	11.96
t_{coll_bat} (s)	324.21	0.21	17.09
Dimensionless parameters			
Ca (-)	9.47E-05	225.81	2.73

λ (-)	0.25	0.25	0.25
$AgNu$ (-)	1.72E-05	381.92	1.98
t_{imm}/t_{coll_bat} (-)	4.42E-06	267.26	1.39

Table 2 shows the agglomerate nucleation number, $AgNu$, for the first model system are very low (i.e. lower than 0.01), thus the time for collision rate limited nucleation is significantly longer than immersion rate limited nucleation. This shows that the kinetics of agglomerate nucleation is limited by the arrival of the particles on the surface of the binder droplet; the immersion of particles inside binder droplets due to interfacial tension forces is so fast and it can be ignored for this system. The system is thus in the *collision rate limited regime* and, therefore, the collision rate limited model is used, with the agglomerate nuclei size evolution with time found by Eqs. (26) and (33) for constant φ_{Pb} (continuous, well mixed, steady state) and batch agglomeration systems, respectively.

Fig. 7 (a) shows that, for the collision rate limited model in a constant φ_{Pb} (continuous, well mixed, steady state) agglomeration system, the size of agglomerate nuclei increases linearly with the agglomeration time until it reaches a maximum size (calculated by $(D_d/2)/\varphi_{cp}$). If we consider the reduction of the crystals in the bulk mother solution, which is typically the case in a batch agglomeration process, the maximum size is reached by an exponential function and over a longer time.

It was assumed in Section 2 that in both models, immersion rate limited and collision rate limited, the agglomerate nucleus grows by formation of a shell of a constant liquid volume

fraction, φ=φ_{cp}, and a core of φ=1. However, we can also calculate an average liquid volume fraction inside the whole volume of agglomerate nucleus, φ_{avg}, as:

$$\varphi_{avg}(t) = \frac{\varphi_{cp}(H_2(t) - H_1(t)) + H_1(t)}{H_2(t)} = \frac{(D_d / 2)}{H_2(t)} \tag{46}$$

where H_2 can be found by Eq. (16) for an immersion rate limited model or Eqs. (26) and (33) for a collision rate limited model. Fig. 7 (b) shows the time evolution of the average liquid volume fraction inside the agglomerate nucleus, φ_{avg}, for model systems 1 which is limited by collision rate. The average liquid volume fraction for both constant φ_{Pb} (continuous, well mixed, steady state) and batch agglomeration systems starts from one, φ_{avg}=1, at t=0 (binder liquid only) and it decreases with the agglomeration time until it drops to φ_{cp} at $t = t_{coll\_cont}$ or t_{coll_bat} for constant φ_{Pb} (continuous, well mixed, steady state) or batch agglomeration system, respectively.

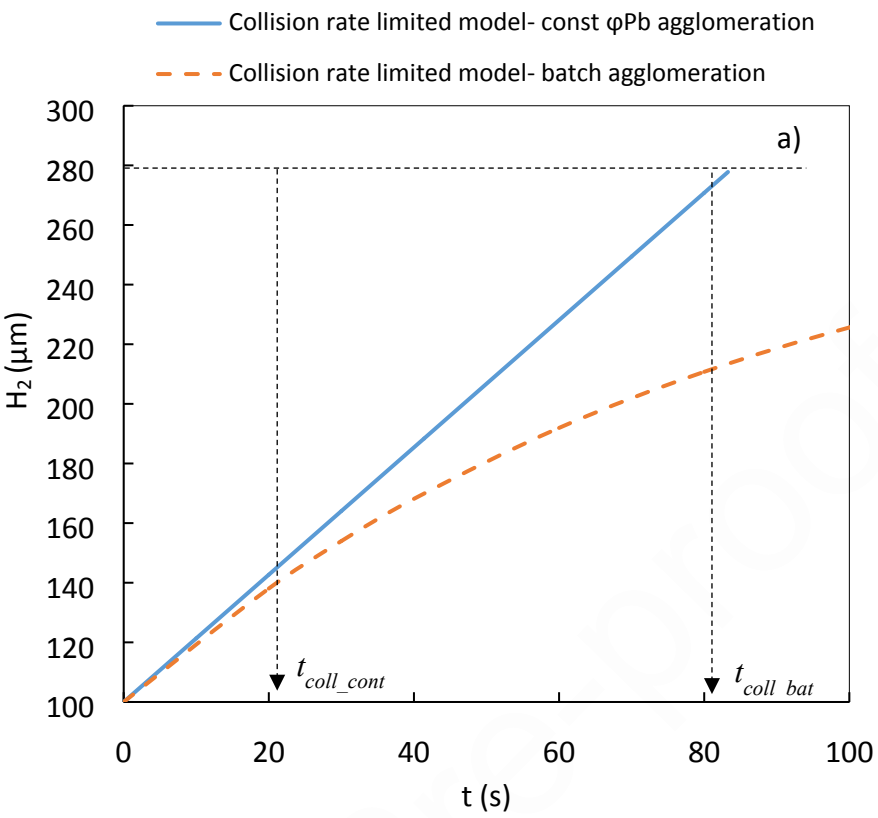
Collision rate limited model- const φPb agglomeration
Collision rate limited model- batch agglomeration
a)
H2 (µm)
300
280
260
240
220
200
180
160
140
120
100
0
20
40
60
80
100
t (s)
t coll_cont
t coll bat

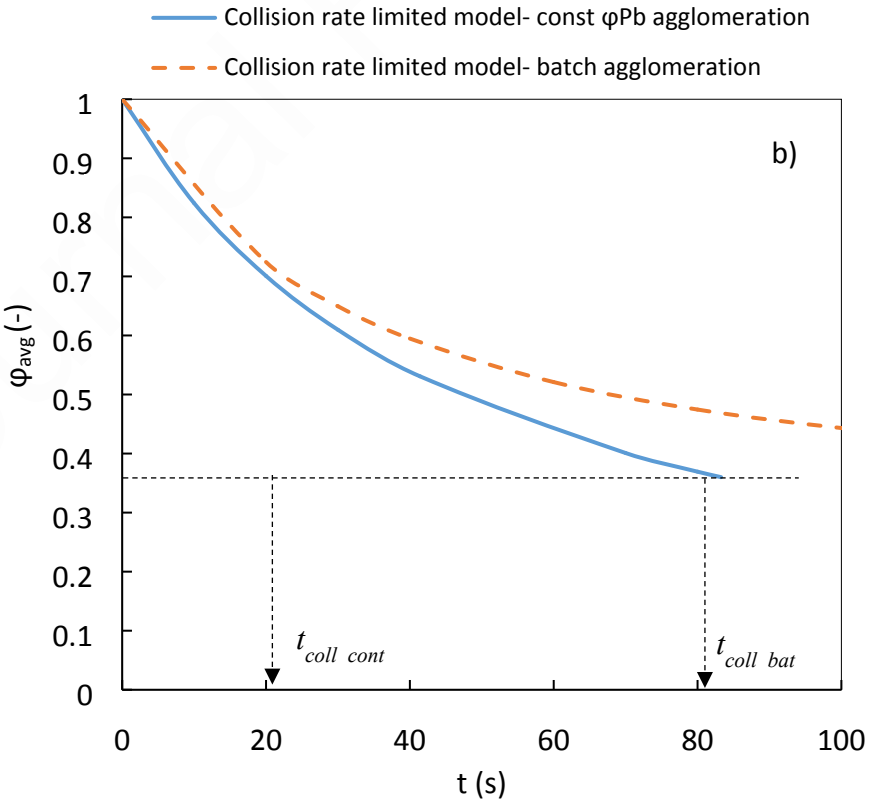
Collision rate limited model- const φPb agglomeration
Collision rate limited model- batch agglomeration
b)
φavg (-)
1
0.9
0.8
0.7
0.6
0.5
0.4
0.3
0.2
0.1
0
0
20
40
60
80
100
t (s)
t coll cont
t coll bat

Fig. 7. Time evolution of agglomerate a) nuclei size and b) average liquid volume fraction for model system 1 limited by collision rate in constant φ_{Pb} and batch agglomeration systems.

In the case of model system 2, the calculation of the $AgNu$ results in a value in the order of magnitudes higher than one (i.e. higher than 100), as well as a longer time for complete agglomerate nucleation limited by immersion rate compared to collision rate limited timescale (Table 2). Accordingly, we can assume that there is always a packed layer of crystals on the surface of the binder droplets and the immersion is controlled by the wetting and suction of crystals inside binder droplets. In this case, the system is in the *immersion rate limited regime* and Eq. (16) is used to determine the time evolution of the agglomerate nuclei size (Fig. 8(a)). In this instance, the size increases to its maximum value as a function of square root of time. Eq. (46) along with Eq. (16) can be used to determine the time evolution of the average liquid volume fraction inside the agglomerate nucleus, φ_{avg} (Fig. 8(b)).

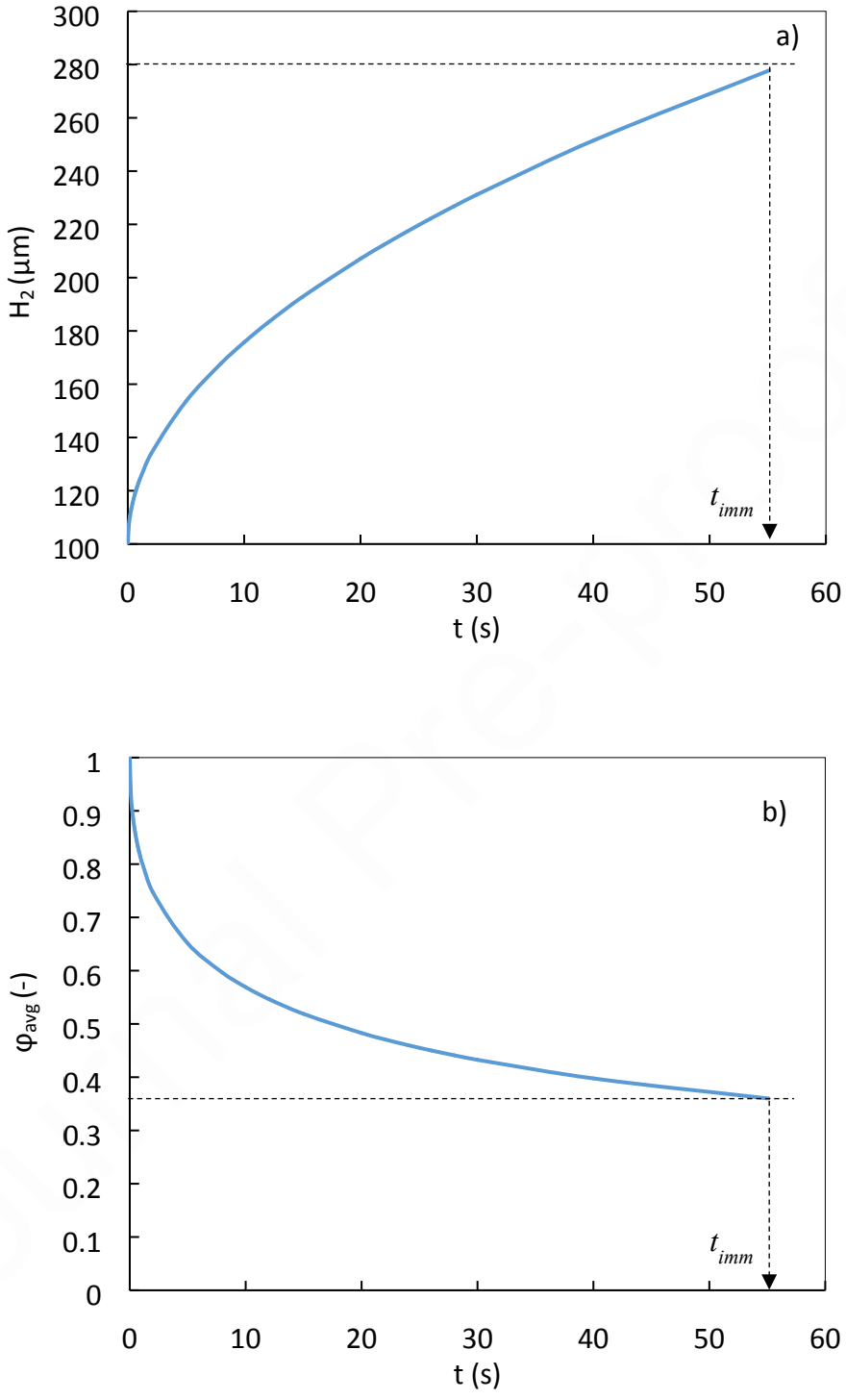

Fig. 8. Time evolution of agglomerate a) nuclei size and b) average liquid volume fraction for model system 2 limited by immersion rate.

However, spherical agglomeration with the formulation properties and process conditions of model system 3 yields an agglomerate nucleation number, $AgNu$, close to 1 and a comparable timescale for both immersion rate and collision rate limited models. Therefore, the system can be limited by both the collision of the crystals to the binder surface and the wetting action for the suction of crystals inside binder droplets. In this case, the system is in an *intermediate regime* and the size of the agglomerate nuclei can be found by a combination of immersion rate and collision rate limited models. Fig. 9(a) shows the time evolution of the agglomerate nuclei size for model system 3, found by both the immersion rate limited model and the collision rate limited model (batch agglomeration system), according to Eq. (16) and Eq. (33), respectively. As can be seen, there is an intersection between the two profiles at time, t_{int}. During initial agglomeration, prior to the time t_{int}, the immersion of crystals inside binder droplets is limited by the collision of particles and the binder droplets, as the wetting suction of crystals inside the binder droplets is faster. Thus, the time evolution of the agglomerate nuclei size can be found by the collision rate limited model until t_{int}. After this time, the rate of collision is faster than the rate of immersion due to surface tension forces. Therefore, the system is limited by the immersion rate, and this model can be utilised to determine the time evolution of the agglomerate nuclei size in the time period of t_{int} to t_{imm}. After finding the time evolution of the agglomerate nucleus size, Eq. (46) can be used to calculate the time evolution of the average liquid volume fraction inside the growing nucleus (Fig. 9(b)). Accordingly, if the agglomerate nucleation number, $AgNu$, is close to one, a combination

of both immersion rate and collision rate limited models can be applied for the kinetics of immersion nucleation in spherical agglomeration.

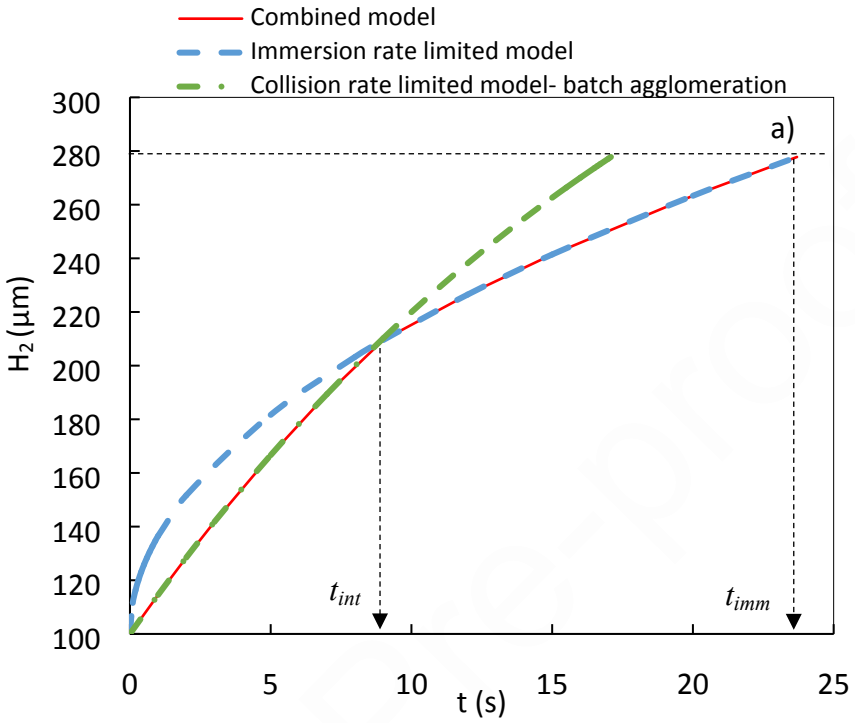

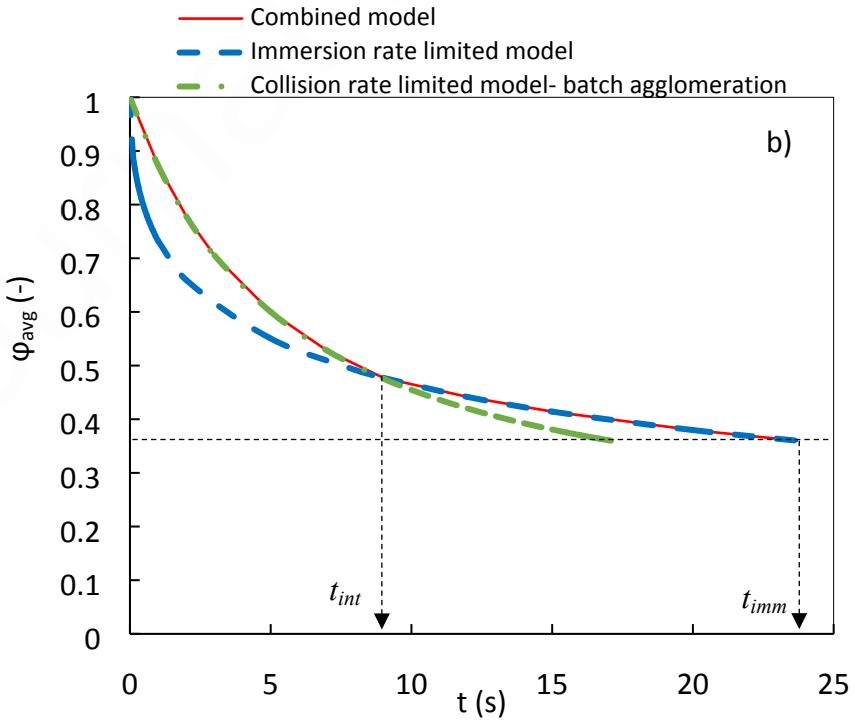

Fig. 9. Time evolution of agglomerate a) nuclei size and b) average liquid volume fraction for model system 3 limited by both collision rate (batch agglomeration system) and immersion rate.

The process of agglomerate nucleation may be limited by the lack of crystal particles in the bulk mother solution. In order to understand the behaviour of the system in such cases, the time evolution of the volume fraction of particles in the bulk mother solution should be determined. A mass conservation of the solid particles within the system resulted in Eq. (31) (Eq. (A3) in Appendix A). Substituting ($H_2(t)$- $H_1(t)$) in Eq. (31) by Eq. (15) or Eq. (32) leads to the following equations for the volume fraction of particles in the bulk mother solution at time moment t:

$$\varphi_{Pb}(t) = \varphi_{Pb0}(1 - \frac{2TBSR}{D_d}(\frac{\Psi D_p \gamma \cos\theta}{15\mu_d}(1-\varphi_{cp})\varphi_{cp}t)^{1/2}) \quad (47)$$

in the case of the immersion rate limited regime and:

$$\varphi_{Pb}(t) = \varphi_{Pb0}\exp(-\frac{2\alpha\left[u(D_p)^2 + u(D_d)^2\right]^{1/2}\varphi_{Pb0}TBSR}{D_d}t) \quad (48)$$

in the case of the collision rate limited regime in a batch agglomeration system.

Calculation of Eq. (47) for model system 2, which is limited by the immersion rate, with various $TBSR$ values, is shown in Fig. 10. As can be seen, at a higher value of $TBSR$ (i.e. 0.7), φ_{Pb} decreases to zero at a time moment, t_{TBSR} shorter than t_{imm}. In this case, there are not enough particles in the bulk mother solution to fill the whole volume of binder droplets

with a particle volume fraction of $(1-\varphi_{cp})$. This scenario happens in a system in which $t_{TBSR} < t_{imm}$. The t_{TBSR} can be calculated from Eq. (47) by replacing $\varphi_{Pb}=0$ as:

$$t_{TBSR} = \frac{15\mu_d D_d^{\,2}}{4\psi D_p \gamma \cos\theta} \frac{1}{TBSR^2 (1-\varphi_{cp})\varphi_{cp}} \tag{49}$$

Eq. (49) shows the timescale for soaking up all the available particles in the bulk mother solution in an immersion rate limited regime. Substituting t_{TBSR} by Eq. (49) and t_{imm} by Eq. (17) in $t_{TBSR} < t_{imm}$ gives the following condition for a system which is limited by the lack of particles in the bulk mother solution:

$$TBSR > \frac{\varphi_{cp}}{(1-\varphi_{cp})} \tag{50}$$

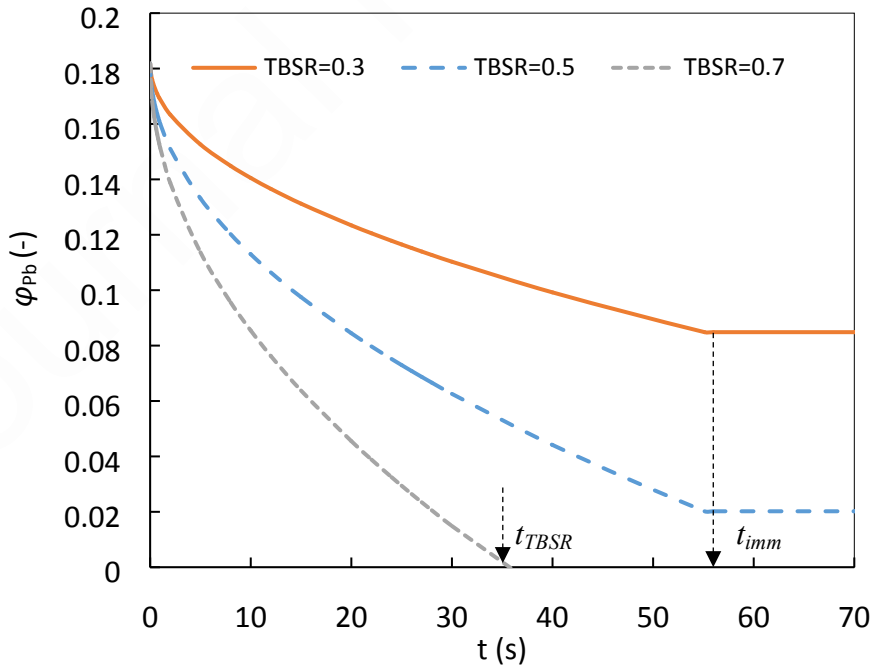

Fig. 10. Time evolution of particle volume fraction in the bulk mother solution for model system 2 (limited by immersion rate in a batch agglomeration system) with various $TBSR$ values.

Fig. 11 shows the time evolution of the particle volume fraction in the bulk mother solution calculated by Eq. (48) for model system 1 (i.e. collision rate limited system) with various $TBSR$ values. As can be seen in Fig. 11 and discussed in section 2.2, for $TBSR$ values higher than $\frac{\varphi_{cp}}{(1-\varphi_{cp})}$ (e.g. $TBSR$=1 in Fig. 11), the particle volume fraction in the bulk mother solution rapidly decreases to very low values and the timescale for complete agglomerate nucleation is infinite due to the lack of particles in the bulk mother solution.

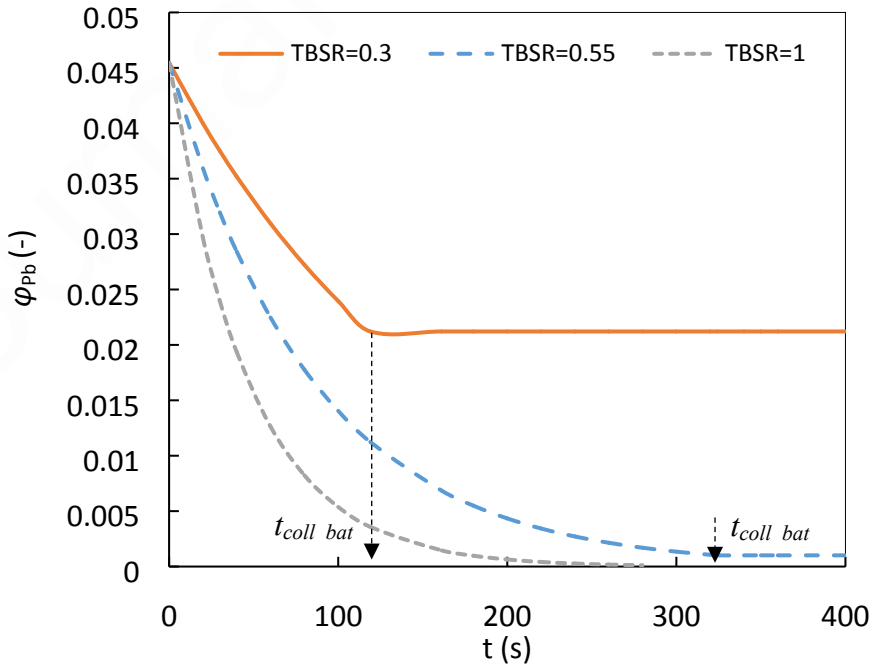

Fig. 11. Time evolution of particle volume fraction in the bulk mother solution for model system 1 (limited by collision rate in a batch agglomeration system) with various $TBSR$ values.

3.2. Sensitivity to formulation properties and process conditions

Fig. 12 and Fig. B.1 (see Appendix B) shows the sensitivity of the model system 1 to the input formulation properties and process conditions. For sensitivity analysis, in each case only one parameter is varied, while all the other inputs are kept constant. As predicted in Section 3.1, model system 1 is limited by collision rate. Therefore, the ranges of the parameters are selected in a way which retain the system in a collision rate limited regime (i.e. agglomerate nucleation number, $AgNu$, lower than 0.01). Eqs. (26) and (33) showed that the following parameters can affect the collision rate limited model, and thus the time evolution of agglomerate nuclei size and timescale for complete nucleation in this regime: D_p, D_d, μ_L, φ_{cp}, ε, φ_{Pb0}, $TBSR$, ρ_p, ρ_d, ρ_L.

- Among these parameters, increasing mean particle size, D_p, critical-packing liquid volume fraction, φ_{cp}, average energy dissipation, ε, and initial crystal content in the bulk mother solution, φ_{Pb0}, results in a shorter nucleation time (Fig. 12 (a), (d), (e) and (f)).
- Conversely, the duration of the nucleation process lengthens with increasing mean binder droplet diameter, D_d, viscosity of mother solution, μ_L, and true binder liquid-to-solid ratio, $TBSR$ (Fig. 12 (b), (c), and (g)).

- At higher values of φ_{cp} and lower values $TBSR$, the change of nuclei size over time is relatively linear in a batch agglomeration system (Fig. 12 (d) and (g)). This behaviour was also observed in Fig. 6(b).
- In the case of ρ_p, ρ_d and ρ_L, there is a non-linear correlation between these parameters and the collision rate between the crystal particles and binder droplets (See Fig. B.1 in Appendix B). This non-linear correlation was described by Eqs. (21)-(23).

The sensitivity of model system 2, which is limited by the immersion rate, to the input parameters is shown in Fig. 13. Similar to Fig. 12, in each case only one parameter is varied, and the ranges of the parameters are selected in a way which retain the system in the reference agglomerate nucleation regime (i.e. an immersion rate limited regime with agglomerate nucleation number, $AgNu$, higher than 100). Fig. 13 shows (and expected from Eq. (16)) that the following parameters can affect the time evolution of agglomerate nuclei size and timescale for complete nucleation in an immersion rate limited regime: D_p, D_d, μ_d, γ, θ, φ_{cp}, Ψ.

- A higher value of D_p, γ, φ_{cp} and Ψ results in a shorter nucleation time (Fig. 12 (a), (d), (f) and (g)) while a longer nucleation time is required with higher values of D_d, μ_d and θ (Fig. 12 (b), (c), and (e)).
- Among these parameters, the timescale of complete nucleation is more sensitive to mean binder droplet diameter, D_d, and critical-packing liquid volume fraction, φ_{cp}, and its sensitivity to binder liquid/solid contact angle, θ, increases as θ approaches to 90º.

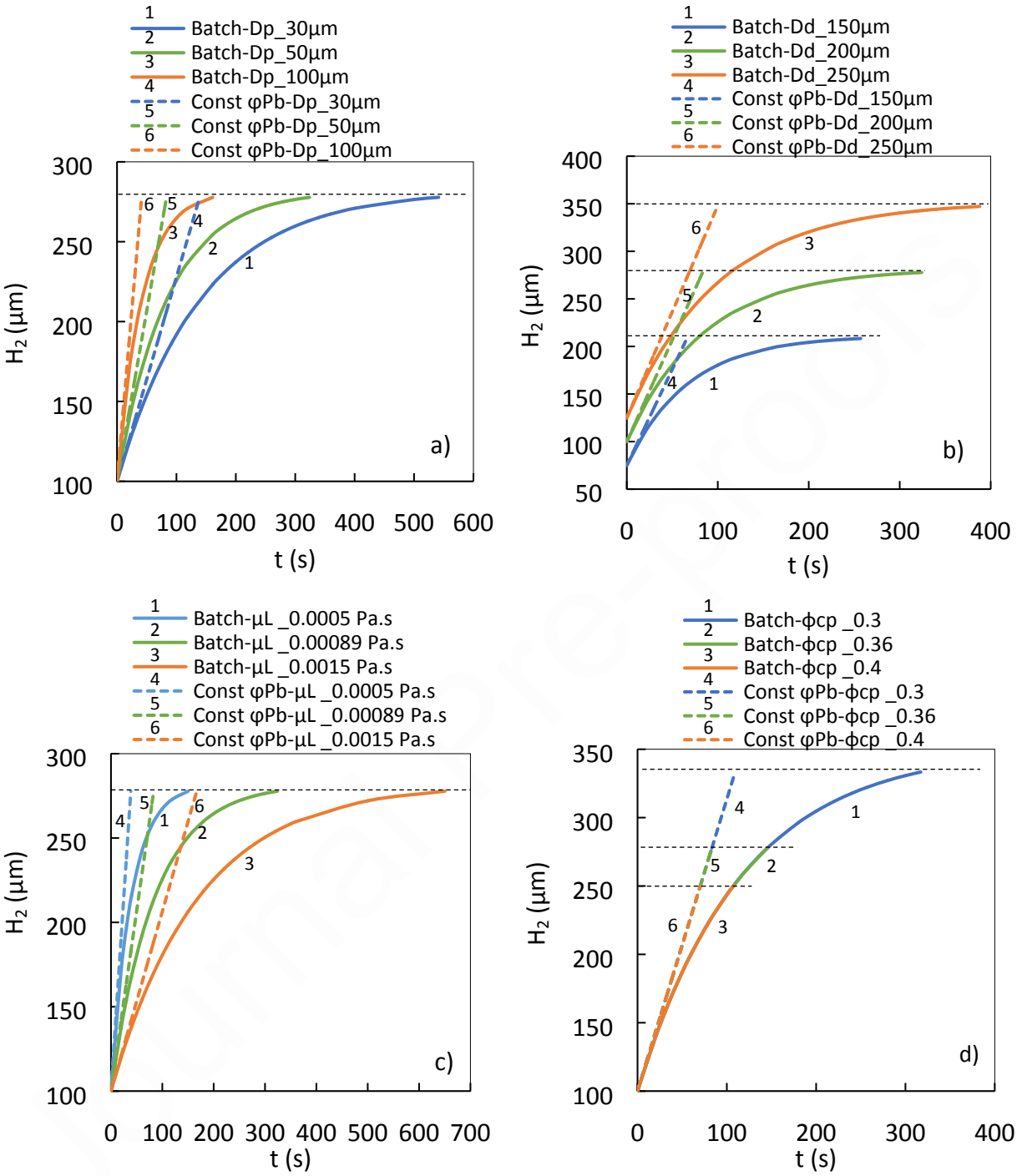
1 Batch-Dp_30µm
2 Batch-Dp_50µm
3 Batch-Dp_100µm
4 Const φPb-Dp_30µm
5 Const φPb-Dp_50µm
6 Const φPb-Dp_100µm
H2 (µm)
t (s)
a)
1 Batch-Dd_150µm
2 Batch-Dd_200µm
3 Batch-Dd_250µm
4 Const φPb-Dd_150µm
5 Const φPb-Dd_200µm
6 Const φPb-Dd_250µm
H2 (µm)
t (s)
b)
1 Batch-µL _0.0005 Pa.s
2 Batch-µL _0.00089 Pa.s
3 Batch-µL _0.0015 Pa.s
4 Const φPb-µL _0.0005 Pa.s
5 Const φPb-µL _0.00089 Pa.s
6 Const φPb-µL _0.0015 Pa.s
H2 (µm)
t (s)
c)
1 Batch-ϕcp _0.3
2 Batch-ϕcp _0.36
3 Batch-ϕcp _0.4
4 Const φPb-ϕcp _0.3
5 Const φPb-ϕcp _0.36
6 Const φPb-ϕcp _0.4
H2 (µm)
t (s)
d)

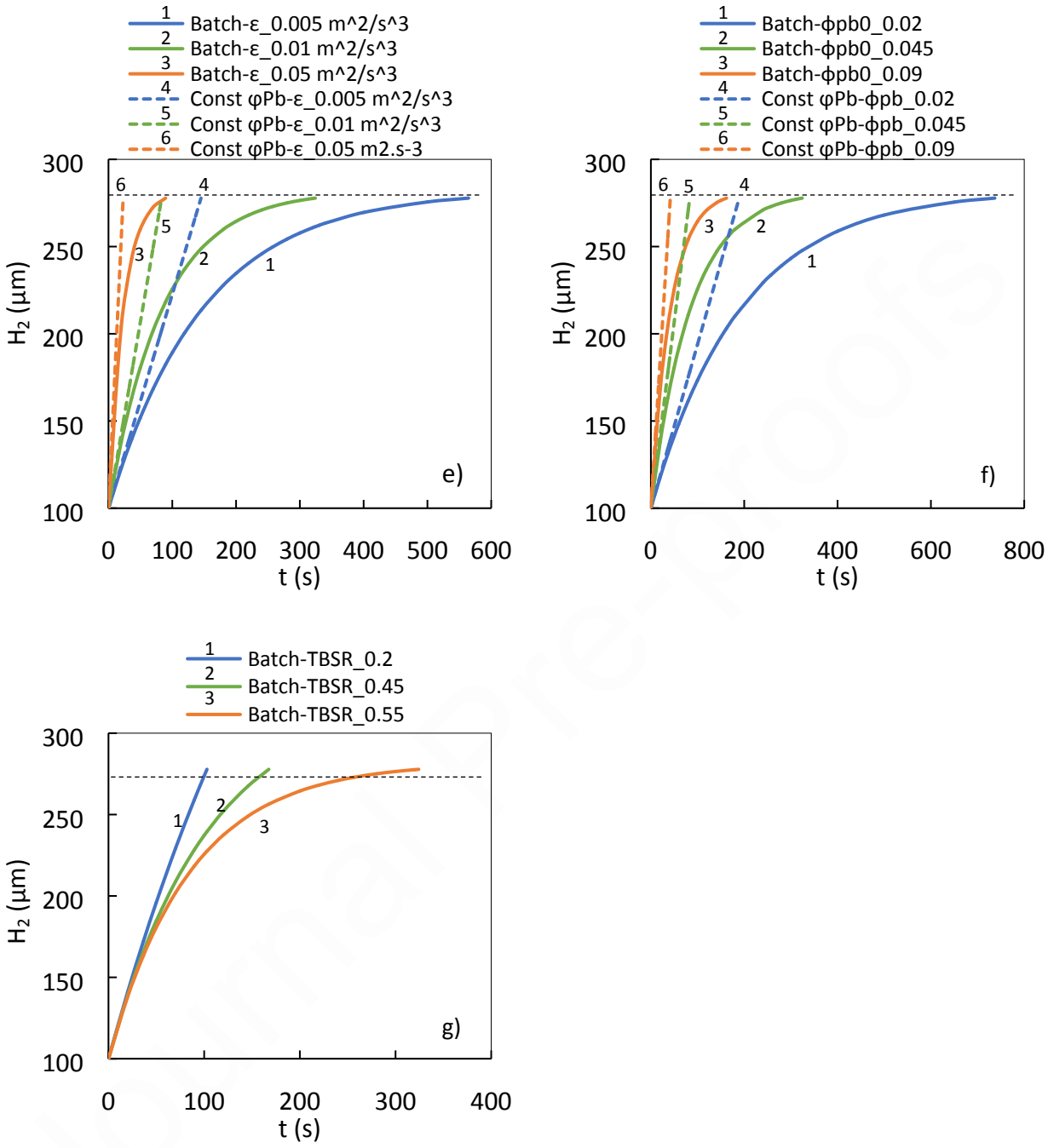

Fig. 12. Sensitivity of time evolution of agglomerate nuclei size to a) mean particle diameter, D_p, b) mean binder droplet diameter, D_d, c) viscosity of mother solution, μ_L, d) critical-packing liquid volume fraction, φ_{cp}, ($TBSR$=0.4), e) average energy dissipation, ε,

f) initial crystal volume fraction in the bulk mother solution, φ_{Pb0}, g) true volumetric binder liquid-to-solid ratio, $TBSR$ for model system 1 limited by collision rate.

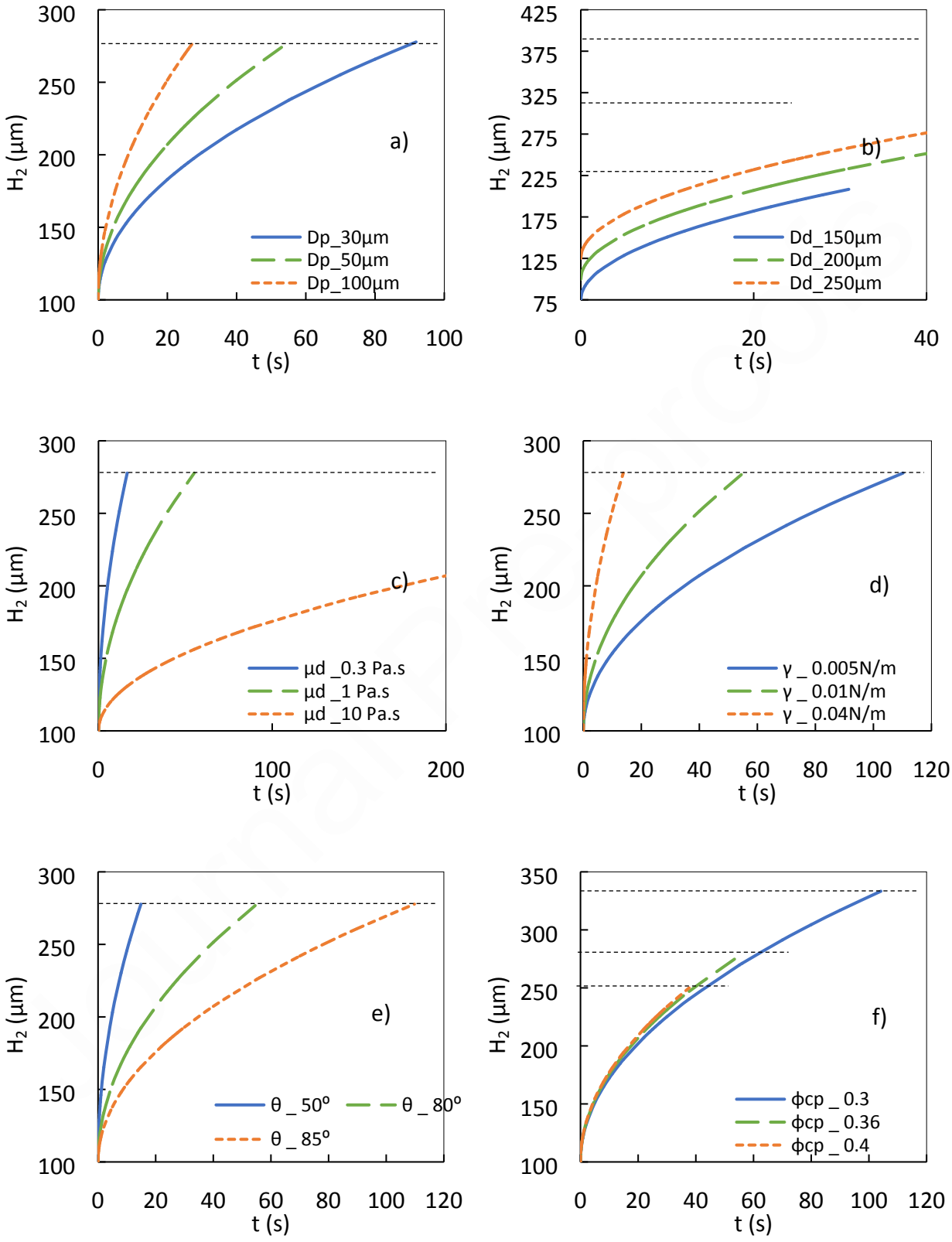
a)
H2 (µm)
t (s)
Dp_30µm
Dp_50µm
Dp_100µm
b)
Dd_150µm
Dd_200µm
Dd_250µm
c)
µd _0.3 Pa.s
µd _1 Pa.s
µd _10 Pa.s
d)
γ _ 0.005N/m
γ _ 0.01N/m
γ _ 0.04N/m
e)
θ _ 50°
θ _ 80°
θ _ 85°
f)
ϕcp _ 0.3
ϕcp _ 0.36
ϕcp _ 0.4

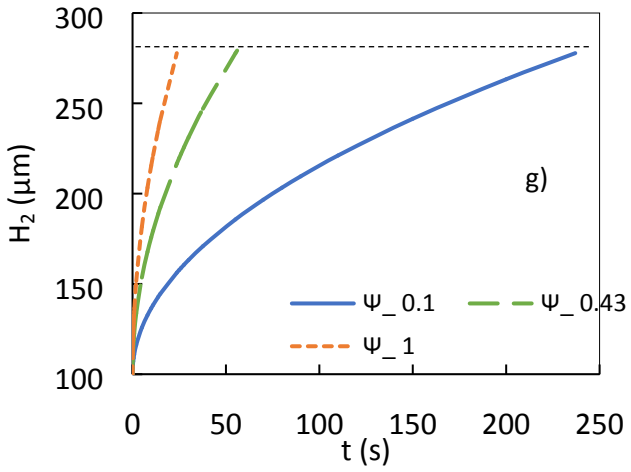

Fig. 13. Sensitivity of time evolution of agglomerate nuclei size to a) mean particle diameter, D_p, b) mean binder droplet diameter, D_d, c) viscosity of the binder liquid, μ_d, d) interfacial tension between binder and mother solution, γ, e) binder liquid/solid contact angle, θ, f) critical-packing liquid volume fraction, φ_{cp}, and g) mean sphericity of crystal particles, Ψ, for model system 2 limited by immersion rate.

Among all formulation and process parameters, only D_d, D_p and φ_{cp} affect the system and the time evolution of agglomerate nuclei in both immersion rate and collision rate limited regimes, however, with different correlations predicted by Eqs. (16), (26) and (33).

Figs. 12 and 13 show that the maximum size of agglomerate nuclei was only affected by the mean binder droplet diameter, D_d, and critical-packing liquid volume fraction, φ_{cp}, (calculated by $(D_d/2)/\varphi_{cp}$) and the other parameters only influence the timescale of complete nucleation. The precise value of φ_{cp} is unknown for crystal particles and it varies mainly with geometrical shape of crystals. Therefore, for a long agglomerate nucleation experiment (i.e. long enough to ensure complete nucleation) the only process parameter,

which dictates the final size of agglomerate nucleus, is the size of binder droplet, D_d, that is, it can be tailored as a design parameter to tune the final size of agglomerate nucleus and size distribution of produced agglomerates in a spherical agglomeration process.

For the realistic model systems presented in Table 2 and analysed in Figs. 12 and 13 by various formulation and process parameters, the predicted timescale for complete agglomerate nucleation does not exceed 10 minutes for both batch and constant φ_{Pb} (continuous, well mixed, steady state) agglomeration systems. The latter is applied for the cases in which enough crystal particles are available in the bulk mother solution. This predicted timescale for agglomerate nucleation is significantly shorter than the crystallisation timescale for most organic molecules. Thus, simultaneous crystallisation and agglomeration can be performed in a single unit operation as a design approach for process intensification. Alternatively, the agglomeration can occur in a small, optimised agglomerator that follows the crystalliser.

Finally, some points should be noted here about the developed mathematical models and their usage for the design of a spherical agglomeration process:

a) Microscopic rearrangements of the primary crystals while they are moving into the centre of droplets or possible jamming of the crystals at the end of the immersion process are not considered in the developed mathematical models for the kinetics of the immersion nucleation. The time scale of such rearrangements and jamming of particles can be negligible compared to the time scale of the immersion for the particles with higher sphericity; however, it may be considerable for the irregularly shaped and needle-like crystals.

b) The mathematical models were developed here for a planar geometry and the volume of an agglomerate nucleus in the planar geometry is proportional to its size. The latter should be taken into account in a direction quantitative comparison between the model predictions and experimental data for agglomerate nucleation. The dimensionless volume derived in Eq. (42) can be a good parameter for such comparison between model results and experimental data.

c) A comprehensive validation of the kinetic models can be achieved by a careful design of a spherical agglomeration experiment in which the immersion is the dominant mechanism for the agglomerate nucleation and the other rate processes, such as agglomeration and breakage, are hindered. Such experimental design and model validation are to be performed in a future work.

d) The new nucleation models can be incorporated in a population balance framework, along with other rate processes, for modelling and optimal design of spherical agglomeration processes.

4. Conclusions

This is the first study to investigate the kinetics of agglomerate nucleation by the immersion mechanism in spherical agglomeration. Immersion rate limited and collision rate limited models have been developed based on mechanistic understanding of the process. The immersion rate limited model assumes that a packed layer of stationary particles is always available on the surface of binder droplets; immersion is limited by the wetting action of these particles through capillary penetration of binder liquid according to

Darcy's law. The collision rate limited model assumes immediate wetting and suction of particles inside binder droplets; the process is limited by the arrival of particles to the binder droplet surface, thus collision rate between these two entities within a turbulent flow. The key conclusions from this work are:

1. Three different regimes for agglomerate nucleation were found to be an *immersion rate limited regime*, a *collision rate limited regime* and an *intermediate regime* in which the system is limited by both the collision rate and immersion rate.
2. A dimensionless group, termed the *agglomerate nucleation number*, was introduced to demarcate the boundary between different regimes of nucleation in spherical agglomeration systems.
3. Agglomerate size was found to increase to its maximum value as a function of the square root of time in an immersion rate limited regime. While, in a collision rate limited regime, the size increases to the maximum value with linear and exponential functions of time for constant φ_{Pb} (continuous, well mixed, steady state) and batch agglomerate systems, respectively.
4. The process of agglomerate nucleation might be limited by the lack of crystal particles in the bulk mother solution. A condition for such a case was identified as a function of true binder liquid-to-solid ratio and critical liquid volume fraction.
5. The predicted timescale for agglomerate nucleation was found to be in the order of a few minutes, which is significantly shorter than typical crystallisation timescales.

Critically, comprehensive understanding of the physics and the influence of both formulation and process parameters is required for the optimal design of spherical

agglomeration processes. This should be achieved in tandem with developing the critical understanding of the process as a whole. The models derived here take a step towards this, as they can be incorporated into population balance models, along with other rate processes, as a means of developing a predictive, robust model for spherical agglomeration.

Acknowledgements

This research was supported by EPSRC Future Continuous Manufacturing and Advanced Crystallisation Research Hub (Grant Ref: EP/P006965/1). The authors are grateful to Dr F. Perciballi, Dr N. Rajoub, Dr C. Brown and Dr I. Houson from University of Strathclyde for sharing insightful experimental data on the spherical agglomeration process and Dr N. Mitchell from Process Systems Enterprise Ltd. (PSE) for perceptive discussions on possible future implementation of the models in process-level population balance model.

Nomenclature

$AgNu$	agglomerate nucleation number defined by Eq. (38)
Ca	modified capillary number defined by Eq. (40)
D_d	average or Sauter mean binder droplet diameter, m
D_p	average or Sauter mean particle diameter, m
g	gravitational acceleration, m/s^2

H_1	radius of the core in planar geometry, m
H_2	radius of the nucleus in planar geometry, m
K	Kozeny's constant
ℓ	length of wetting liquid displacement, m
N_{sep}	separation number
P	pressure, Pa
q	volumetric flow rate, m^3/s
Q	volumetric flux, m/s
Q_{coll}	collision rate of small crystals with a binder droplet, m/s
Q_{imm}	rate of particle immersion inside a binder droplet, m/s
r	radial co-ordinate, m
R	radius of the pipe/capillary, m
R_{eff}	effective radius of the pores for the packed layer of particles, m
S_v	specific surface area per unit volume, 1/m
t	time, s
t_{coll_bat}	time for complete agglomerate nucleation limited by collision rate in a batch agglomeration system, s

t_{coll_cont} time for complete agglomerate nucleation limited by collision rate in a constant φ_{Pb} (continuous, well mixed, steady state) agglomeration system, s

t_{imm} time for complete agglomerate nucleation limited by immersion rate, s

t_{int} time of intersection between immersion rate and collision rate limited models, s

u velocity, m/s

$u(D_d)$ binder droplet-mother solution relative velocity, m/s

$u(D_p)$ particle-mother solution relative velocity, m/s

$u_t(D_P)$ crystal particles terminal velocity, m/s

z co-ordinate axis, m

Greek Symbols

α target efficiency

ε average energy dissipation per unit of suspension mass, m^2/s^3

γ interfacial tension between binder and mother solution solution, N/m

κ permeability for the packed layer of particles, m^2

λ ratio of the particle size to the binder droplet size

μ_d viscosity of the binder liquid, Pa s

μ_L	viscosity of the mother solution, Pa s
φ	liquid volume fraction
φ_{avg}	average liquid volume fraction inside agglomerate nucleus
φ_{cp}	critical-packing liquid volume fraction
φ_{Pb}	particle volume fraction in the bulk mother liquid
φ_{Pb0}	initial particle volume fraction in the bulk mother liquid
θ	binder liquid/solid contact angle at three-phase binder liquid/mother solution/solid contact line, radians
ρ_d	density of the binder liquid, kg/m^3
ρ_L	density of the mother solution, kg/m^3
ρ_p	skeletal density of crystal particles, kg/m^3
τ_{coll_bat}	dimensionless time for complete agglomerate nucleation limited by collision rate in a batch agglomeration system
τ_{coll_cont}	dimensionless time for complete agglomerate nucleation limited by collision rate in a constant φ_{Pb} (continuous, well mixed, steady state) agglomeration system
τ_{imm}	dimensionless time for complete agglomerate nucleation limited by immersion rate
ψ	dimensionless size or volume

ψ_{coll_bat} dimensionless size or volume for collision rate limited model in a batch agglomeration system

ψ_{coll_cont} dimensionless size or volume for collision rate limited model in a constant φ_{Pb} (continuous, well mixed, steady state) agglomeration system

ψ_{imm} dimensionless size or volume for immersion rate limited model

Ψ sphericity factor for crystal particles

ζ dimensionless co-ordinate axis

ζ_1 dimensionless radius of the core in planar geometry

ζ_2 dimensionless radius of the nucleus in planar geometry

ξ coefficient defined by Eq. (23), 1/s

References

Amaro-González, D., Biscans, B., 2002. Spherical agglomeration during crystallization of an active pharmaceutical ingredient. Powder Technology 128 (2-3),188-194. https://doi.org/10.1016/S0032-5910(02)00196-1

Barera-Medrano, D., Reynolds, G.K., Bonsall, J., Salman, A.D., Hounslow, M.J., 2006. An X-ray tomography study of the effect of processing time on granule structure in high shear melt granulation, AIChE Spring National Meetin, Orlando, FL.

Bird, R.B., Stewart, W.E., Lightfoot, E.N., 2007. Transport Phenomena. John Wiley & Sons.

Blandin, A., et al., 2003. Agglomeration in suspension of salicylic acid fine particles: influence of some process parameters on kinetics and agglomerate final size. Powder Technology 130(1-3), 316-323. https://doi.org/10.1016/S0032-5910(02)00210-3

Blandin, A., et al., 2005. Modelling of agglomeration in suspension: Application to salicylic acid microparticles. Powder Technology 156(1), 19-33. https://doi.org/10.1016/j.powtec.2005.05.049

Bos, A.S., 1983. Agglomeration in suspension, Doctoral thesis, Delft University of Technology

Bouwman, A.M., Henstra, M.J., Westerman, D., Chung, J.T., Zhang, Z., Ingram, A., Seville, J.P.K., Frijlink, H.W., 2005. The effect of the amount of binder liquid on the granulation mechanisms and structure of microcrystalline cellulose granules prepared by high shear granulation, International Journal of Pharmaceutics 290(1–2), 129-136. https://doi.org/10.1016/j.ijpharm.2004.11.024

David, R., et al., 1991. Crystallization and precipitation engineering—III. A discrete formulation of the agglomeration rate of crystals in a crystallization process. Chemical Engineering Science 46(1), 205-213. https://doi.org/10.1016/0009-2509(91)80130-Q

David, R., et al., 2003. Modelling of multiple-mechanism agglomeration in a crystallization process. Powder Technology 130(1-3), 338-344. https://doi.org/10.1016/S0032-5910(02)00213-9

Hounslow, M., Oullion, M., Reynolds, G., 2009. Kinetic models for granule nucleation by the immersion mechanism. Powder Technology 189(2), 177-189. https://doi.org/10.1016/j.powtec.2008.04.008

Iveson, S.M., et al., 2001. Nucleation, growth and breakage phenomena in agitated wet granulation processes: a review. Powder Technology 117(1-2), 3-39. https://doi.org/10.1016/S0032-5910(01)00313-8

Kawashima, Y. Capes, C., 1976. Further studies of the kinetics of spherical agglomeration in a stirred vessel. Powder Technology 13(2), 279-288. https://doi.org/10.1016/0032-5910(76)85014-0

Kawashima, Y., Okumura, M., Takenaka, H., 1982. Spherical crystallization: direct spherical agglomeration of salicylic acid crystals during crystallization. Science 216(4550), 1127-1128. https://doi.org/10.1126/science.216.4550.1127

Kuboi, R., Nienow, A., Conti, R., 1984. Mechanical attrition of crystals in stirred vessels. Industrial Crystallization 84, 211-216.

Kumar, S., Chawla, G., Bansal, A.K., 2008. Spherical crystallization of mebendazole to improve processability. Pharmaceutical Development and Technology 13(6), 559-568. https://doi.org/10.1080/10837450802310180

Lee, D.-G., Kim, H.-Y., 2008. Impact of a superhydrophobic sphere onto water. Langmuir 24(1), 142-145. https://doi.org/10.1021/la702437c

Litster, J., 2016. Design and Processing of Particulate Products. Cambridge University Press.

Madec, L., Falk, L., Plasari, E., 2003., Modelling of the agglomeration in suspension process with multidimensional kernels. Powder Technology 130(1-3), 147-153. https://doi.org/10.1016/S0032-5910(02)00258-9

Müller, M., Löffler, F., 1996. Development of agglomerate size and structure during spherical agglomeration in suspension. Particle & Particle Systems Characterization 13(5), 322-326. https://doi.org/10.1002/ppsc.19960130512

Ochsenbein, D.R., et al., 2015. Agglomeration of needle-like crystals in suspension. II. Modeling. Crystal Growth & Design 15(9), 4296-4310. https://doi.org/10.1021/acs.cgd.5b00604

Orlewski, P.M., Ahn, B., Mazzotti, M., 2018. Tuning the Particle Sizes in Spherical Agglomeration. Crystal Growth & Design 18(10), 6257-6265. https://doi.org/10.1021/acs.cgd.8b01134

Peña, R., et al., 2017. Modeling and optimization of spherical agglomeration in suspension through a coupled population balance model. Chemical Engineering Science 167, 66-77. https://doi.org/10.1016/j.ces.2017.03.055

Perciballi, F., 2017. Formation of optimised particles for formulation and processing. Doctoral thesis. University of Strathclyde.

Pitt, K., et al., 2018. Particle design via spherical agglomeration: A critical review of controlling parameters, rate processes and modelling. Powder Technology 326, 327-343. https://doi.org/10.1016/j.powtec.2017.11.052

Reay, D., Ramshaw, C., Harvey, A., 2008. Process Intensification: Engineering for efficiency, sustainability and flexibility. Butterworth-Heinemann.

Schæfer, T., Mathiesen, C., 1996. Melt pelletization in a high shear mixer. IX. Effects of binder particle size. International Journal of Pharmaceutics 139(1-2), 139-148. https://doi.org/10.1016/0378-5173(96)04548-6

Sirianni, A., Capes, C., Puddington, J., 1969. Recent experience with the spherical agglomeration process. The Canadian Journal of Chemical Engineering 47(2), 166-170. https://doi.org/10.1002/cjce.5450470212

Subero-Couroyer, C., et al., 2006. Agglomeration in suspension of salicylic acid fine particles: Analysis of the wetting period and effect of the binder injection mode on the final agglomerate size. Powder Technology 161(2), 98-109. https://doi.org/10.1016/j.powtec.2005.08.014

Sutherland, J., 1962. The agglomeration of aqueous suspensions of graphite. The Canadian Journal of Chemical Engineering 40(6), 268-272. https://doi.org/10.1002/cjce.5450400609

Usha, A.N., et al., 2008. Preparation and, in vitro, preclinical and clinical studies of aceclofenac spherical agglomerates. European Journal of Pharmaceutics and Biopharmaceutics 70(2), 674-683. https://doi.org/10.1016/j.ejpb.2008.06.010

White, L.R., 1982. Capillary rise in powders. Journal of Colloid and Interface Science 90(2), 536-538. https://doi.org/10.1016/0021-9797(82)90319-8

Appendix A

A mass conservation of the solid particles within the system can be given as:

$$2n_d A(1-\varphi_{cp})(H_2(t)-H_1(t))+\varphi_{Pb}(t)V_{tot}=\varphi_{Pb0}V_{tot} \quad \text{(A1)}$$

where n_d is the number of binder droplets; A is the cross-sectional area of binder droplet in planar geometry; V_{tot} is the total volume of the system; φ_{Pb0} and $\varphi_{Pb}(t)$ are particle volume fractions in the bulk mother solution at $t=0$ and time moment t.

Replacing n_d in the above equation by $V_{tot\_d}/A.D_d$ gives:

$$2\frac{V_{tot\_d}}{AD_d}A(1-\varphi_{cp})(H_2(t)-H_1(t))+\varphi_{Pb}(t)V_{tot}=\varphi_{Pb0}V_{tot} \quad \text{(A2)}$$

where V_{tot_d} is the total volume of binder droplets.

Rearranging Eq. A2 and replacing V_{tot_d}/V_{tot} by $TBSR.\varphi_{Pb0}$ gives the following equation for the volume fraction of particles in the bulk mother solution at time moment t:

$$\varphi_{Pb}(t)=\varphi_{Pb0}(1-\frac{2TBSR}{D_d}(1-\varphi_{cp})(H_2(t)-H_1(t))) \quad \text{(A3)}$$

where $TBSR$ is the true volumetric binder liquid-to-solid ratio.

Appendix B

The sensitivity of model system 2, which is limited by the immersion rate, to the densities of crystal particles, ρ_p, the binder liquid, ρ_d, and the mother solution, ρ_L is shown in Fig. B.1. As described by Eqs. (21)-(23), there is a non-linear correlation between these parameters and the collision rate between the crystal particles and binder droplets (thus the agglomerate nuclei size over time, and timescale for complete nucleation). As for the effect of ρ_p or ρ_d, the relative value of these parameters against ρ_L should also be considered (i.e. $|\rho_p-\rho_L|$ or $|\rho_d-\rho_L|$). In the case of varying ρ_L, values of both $|\rho_p-\rho_L|$ and $|\rho_d-$

$\rho_L|$ also affect the collision rate, agglomerate nuclei size, and timescale of complete nucleation. These effects can be seen in Fig. B.1 for different values of ρ_p, ρ_d and ρ_L.

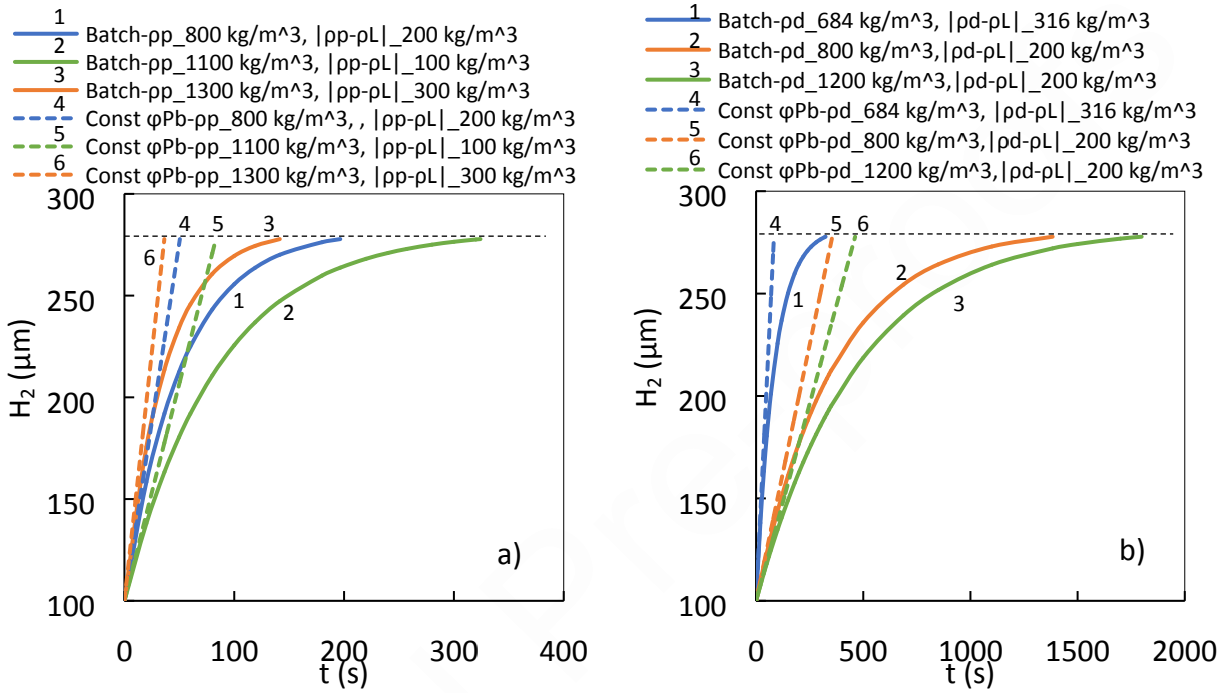

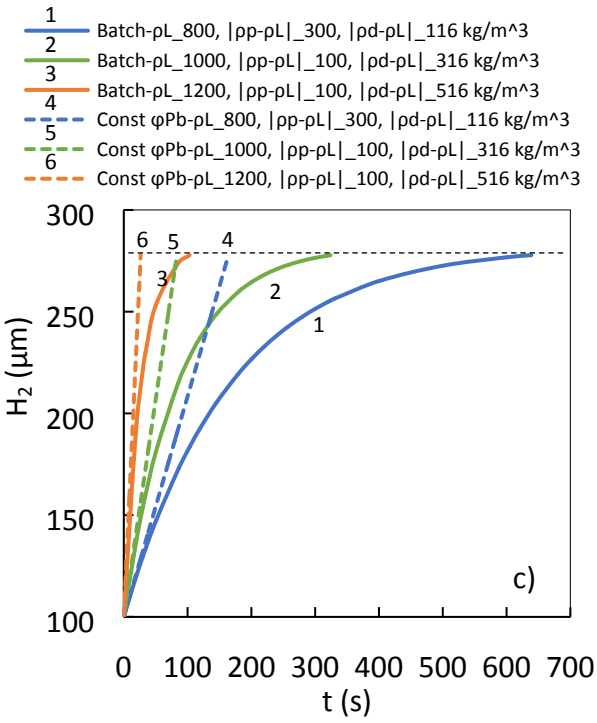

Fig. B.1. Sensitivity of time evolution of agglomerate nuclei size to a) density of crystal particles, ρ_p, b) density of the binder liquid, ρ_d, and c) density of the mother solution, ρ_L for model system 1 limited by collision rate.

- Mathematical models introduced for agglomerate nucleation by immersion mechanism
- 3 regimes identified: immersion rate limited, collision rate limited, intermediate
- A dimensionless group, agglomerate nucleation number, predicts the regimes
- Time evolution of nucleus size and average liquid volume fraction predicted
- Predicted timescale for agglomerate nucleation in the order of a few minutes

Declaration of interests

☒ The authors declare that they have no known competing financial interests or personal relationships that could have appeared to influence the work reported in this paper.

☐The authors declare the following financial interests/personal relationships which may be considered as potential competing interests: